EFFCTS OF THE CANCER AND MUSCLE GROWTH ON LIPID METABOLISM IN ADIPOSE TISSUE AND SKELETAL MUSCLE

Juulia Lautaoja

Master´s thesis in Exercise Physiology
Spring 2017

Faculty of Sport and Health Sciences
University of Jyväskylä
Research supervisors: Juha Hulmi & Tuuli Nissinen
Seminar supervisor: Heikki Kainulainen

ABSTRACT

Lautaoja, Juulia 2017. Effects of the cancer and muscle growth on lipid metabolism in adipose tissue and skeletal muscle. Faculty of Sport and Health Sciences, University of Jyväskylä, Master's thesis in Exercise Physiology**,** 79 pp.

Introduction. Cancer cachexia affects multiple cancer patients by wasting the adipose tissue and skeletal muscle. Weight loss of the cachectic patients decreases survival expectancy and tolerance to the anti-cancer treatments thus lowering the quality of life. Adipose tissue atrophy is associated with white adipose tissue (WAT) browning which enhances the thermogenic ability of the white adipocytes to release energy as heat. This theory has recently been criticized and the aim of this study is to determine if WAT browning does occur in the early cachexia. Secondly, we investigate if triacylglycerol (TG) accumulate into skeletal muscle in early cachexia. Blockade of the ACVR2B pathway by it soluble form, sACVR2B-Fc, is shown to maintain lean mass without preventing adipose tissue atrophy. In this study, we also determine the effects of this treatment on lipid metabolism in adipose tissue and skeletal muscle.

Methods. Colon-26 carcinoma (C26) tumor-bearing BALB/c mice were used in the study. The mice were randomized to healthy control group (CTRL, n = 9), placebo treatment group (C26 + PBS, n = 9) or two of the groups receiving sACVR2B-Fc treatment, either to the continued treatment group (C26 + ACVR c, n = 9) or only before C26 inoculation treated group (ACVR b, n = 9). WAT browning markers, mitochondrial function, lipolysis and lipogenesis as well as inflammation signaling were determined by Western blot protein analysis and/or RT-qPCR. Intramyocellular TG content was measured by Konelab device.

Results. Signs of enhanced WAT browning markers at protein level were not observed in subcutaneous white adipose tissue (scWAT), and only slight increases at mRNA level suggesting that WAT browning may not occur in early cachexia. C26 caused significant adipose tissue atrophy via some other pathway(s) without additional effect of the sACVR2B-Fc treatment. Lipolysis and lipogenesis remained unaltered in early cachexia with a decreasing trend in mitochondrial protein levels. Accumulation of TGs into skeletal muscle was not observed in early cachexia without any effect of sACVR2B-Fc treatment.

Conclusions. These observations support the less significant role of WAT browning on adipose tissue wasting in cancer cachexia. Lipid accumulation into skeletal muscle may not occur in early cachexia due to normal mitochondrial markers. sACVR2B-Fc treatment has no effect on lipid metabolism in adipose tissue or skeletal muscle in early cachexia

Key words: sACVR2B-Fc, C26 tumor-bearing mice, cancer cachexia, lipid accumulation, tissue wasting, WAT browning

ACKNOWLEDGEMENTS

There have been multiple valuable people helping me on this journey of writing my thesis. This would not have been possible without you so I want to raise a few names from whom I have learnt the most of scientific work. Firstly, I want to thank my supervisors Juha Hulmi and Tuuli Nissinen for all your time, patience and advices along this project and letting me take part in this interesting field of research. Secondly, I want to thank Jaakko Hentilä and Aila Ollikainen for helping me with multiple steps during the collection and analyzes of the data. You all have been a significant help to me and given me the confident in myself as a scientist.

Without the support I have received from home I maybe would not have had the courage to switch from biochemistry to exercise physiology. For this, big thanks go to my parents Marja and Heikki for always believing me and supporting my decisions. Last, but not least I want to thank Janne, a person who has been the sound of sense during this year and the reminder of other valuable things in life.

ABBREVIATIONS

AAV	Adeno-associated virus
ACIP	AMPK-stabilizing peptide
ACC	Acetyl CoA carboxylase
ActA	Activin A
ACVR2B/A	Activin receptor type 2B and 2A
ACVR b/c	Check C26 + ACVR b/c
AKT	Protein kinase B
AMPK	AMP-activated protein kinase
ATGL	Adipose triglyceride lipase
ATP	Adenosine triphosphate
BAT	Brown adipose tissue
C26	Colon-26 carcinoma
C26 + PBS	C26 cancer group treated with PBS
C26 + ACVR b	C26 cancer group treated with sACVR2B-Fc before C26
C26 + ACVR c	C26 cancer group treated continuously with sACVR2B-Fc
cDNA	Complementary DNA
CIDEA	Cell death-inducing DFFA-like effector A
CTRL	Control study group
cAMP	Cyclic adenosine monophosphate
CS	Citrate synthase
DAG	Diacylglycerol
DIO2	Type II iodothyronine deiodinase
EPA	Eicosapentaenoic acid
eWAT	Epididymal white adipose tissue
FFA(s)	Free fatty acid(s)
FOXO3a	Forkhead box O3a
GA	Gastrocnemius muscle
GAPDH	Glyceraldehyde 3-phosphate dehydrogenase
GLUT4	Glucose transporter type 4
HSL	Hormone sensitive lipase
IL-6	Interleukin 6
iWAT	Inguinal white adipose tissue
LLC	Lewis lung carcinoma
MAG	Monoacylglycerol
MAGL	Monoacylclycerol lipase
mRNA	Messenger RNA
miRNA	Micro RNA
mTOR	Mammalian target of rapamycin
mTORC1/mTORC2	Mammalian target of rapamycin complex 1/2
MuRF1	Muscle RING-finger protein 1

NAD^+	Oxidized nicotinamide adenine dinucleotide
NADH	Reduced nicotinamide adenine dinucleotide
OXPHOS	Subunits of the respiratory chain
PGC-1α	Peroxisome proliferator-activated receptor γ coactivator 1α
PLIN3 or 5	Perilipin 3 or 5
PKA	Protein kinase A
PPRARγ	Peroxisome proliferator-activated receptor γ
PTH	Parathyroid hormone
PTHrP	Parathyroid hormone-related protein
PRDM16	PR domain containing 16
PUFA	Polyunsaturated fatty acid
Rn18S	18S ribosomal RNA
RNA	Ribonucleic acid
RPLP0, a.k.a 36B4	Ribosomal phosphoprotein P0
RT-qPCR	Real-time quantitative polymerase chain reaction
sACVR2B-Fc	Soluble ligand binding domain of ACVR2B fused to the Fc domain of IgG
scWAT	Subcutaneous white adipose tissue
Smad2	Smad family member 2
STAT3	Signal transducer and activator of transcription 3
TA	Tibialis anterior muscle
TBP	TATA-box binding protein
TG(s)	Triglyceride(s)
TGF-β	Transforming growth factor-β
UCP1	Uncoupling protein 1
VO_2	Oxygen uptake
vWAT	Visceral white adipose tissue
WAT	White adipose tissue

CONTENTS

1 INTRODUCTION

Cancer kills millions of people worldwide every year making it a second most common cause of death in 2013 and the number is growing fast e.g. due to ageing and growing population (Naghavi et al. 2015). Cachexia is related to many cancers and it decreases treatment tolerance and survival expectancy of the patients. Cachexia causes involuntary tissue wasting which cannot be treated with nutritional support. (Acharyya et al. 2004; Petruzzelli et al. 2016). At the moment, there is no cure for cancer cachexia.

If body weight and skeletal muscle mass are maintained during cachexia, tolerance to anti-cancer therapies increases and prognosis for survival improves. Blocking of the Activin receptor type 2B (ACVR2B) pathway inhibits the effects of myostatin and activins thus preventing muscle mass loss without effecting adipose tissue wasting rate (Zhou et al. 2010).

sACVR2B-Fc is a recombinant protein which is composed of the human ectodomain of ACVR2B and human IgG1 Fc domain to produce required fusion protein (Hulmi et al. 2013). This soluble protein will bind to ACVR2B receptor and block the actions of transforming growth factor-β (TGF-β) family members like Activin A (ActA) and myostatin in the circulation. Therefore, the contractile proteins of the skeletal muscle are spared from ubiquitination and proteolysis and muscle mass will remain the same or even increase in cancer cachexia. This stabilization of the body weight has been shown to be important to survival. (Zhou et al. 2010). Usage of sACVR2B-Fc treatment may enhance white adipose tissue (WAT) browning and adipose tissue wasting during cachexia thus changing the body composition of the cachectic patients. (Shan et al. 2013; Tsuchida 2014).

Based on this information there are two aims for this thesis. The primary aim is to study WAT browning markers in early cachexia and determine if sACVR2B-Fc treatment alters the gene expression of WAT browning regulators. The secondary aim is to determine if triacylglycerol accumulates into skeletal muscle in early cachexia and determine the effect of sACVR2B-Fc administration on lipid storage in skeletal muscle.

2 CANCER CACHEXIA

Cancer cachexia is a multi-organ disease that significantly decreases the curability of the patients, at least in part due to a lowered tolerance to anti-cancer treatments (Kir et al. 2014). Many cancers are featured with cachectic symptoms such as adipose tissue wasting and skeletal muscle loss. Atrophy of the skeletal muscle can occur with or without the loss of the adipose tissue deposits (Evans et al. 2008; Bossola et al. 2016). Loss of the adipose tissue can also occur even in the absence of the muscle loss in cancer patients (Tsoli et al. 2015).

2.1 Definition and features of cancer cachexia

Most human cancers will at some point develop a state called cancer cachexia (Greek: kakós hexis – bad condition). Cancer cachexia affects about 80 % and is the cause of death of 15-30 % of the all cancer patients with advanced state of the disease (Zhou et al. 2010; Das et al. 2011; Chen et al. 2014; Petruzzelli et al. 2014). Cancer cachexia is a metabolic syndrome that has symptoms of anorexia, anemia, increased lipolysis, insulin resistance and systemic inflammation (Acharyya et al. 2004; Petruzzelli et al. 2016). This disease tremendously decreases the quality of life of the cancer patients by wasting white WAT and skeletal muscle leading to significant involuntary weight loss independently of nutritional support (Petruzzelli et al. 2014). Loss of the adipose tissue occurs in the very early state of the cachexia as it is observed even prior to a noticeable tumor (Petrzzelli & Wanger 2016).

On average, extremely cachectic patients have been estimated to lose 32 % of their original body weight accompanied with skeletal muscle loss by 75 % and adipose tissue loss by 85 % (Das & Hoefler 2013). By these means cachexia could be referred as “autocannibalism” as while other tissues are wasted the tumor survives (Fearon et al. 2012). Additionally, the size of the tumor is unrelated to severity of cancer cachexia as usually small tumors, e.g. pancreatic tumor, cause more wasting than larger tumors (Petruzzelli & Wagner 2016). Also, the type and location of the tumor affects the severity of cancer cachexia as sarcomas and breast cancer cause only small weight loss whereas pancreatic and gastric cancers cause significant weight loss to 80-90 % of the patients (Tsoli & Robertson 2013).

One other feature of the cachexia is that it may lower the appetite and food intake and lead to negative protein and energy balance that cannot be overcome by nutritional supplementation to stop the wasting phenomenon (Das et al. 2011; Penet & Bhujwalla 2015). These individuals have reduced ability to tolerate given treatments, response to anti-cancer therapies and they have lowered survival rate (Kir et al. 2014). Figure 1 illustrates the complexity of cancer cachexia as it affects multiple different organs via multiple pathways and mediators.

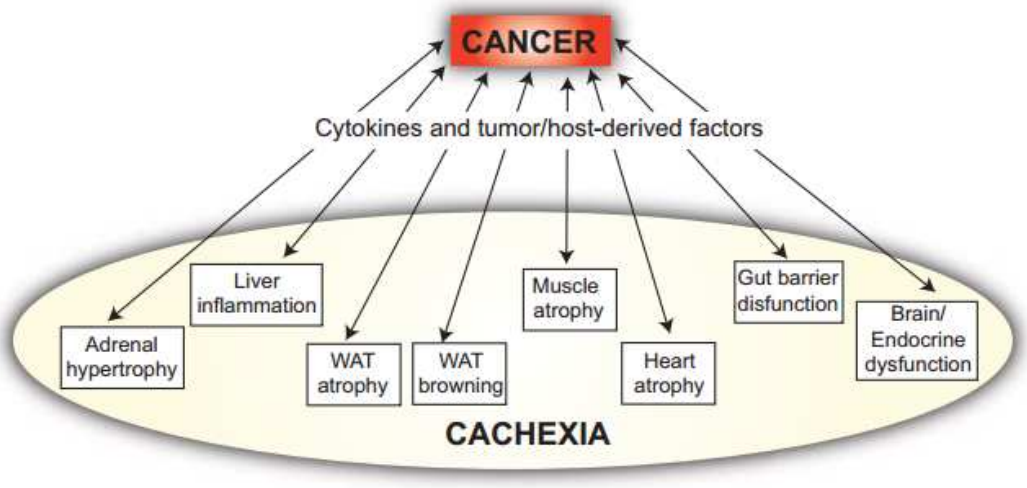

FIGURE 1. Metabolic impairments of various tissues and organs feature the progression of cancer cachexia. Cancer cachexia is a multi-organ disease and abnormal function of e.g. the skeletal muscle, adipose tissue, liver and heart can be observed in cachectic patients. (Petruzzelli & Wagner 2016).

Cancer cachexia can be divided to three stages by its progression; milder precachexia, cachexia and severe refractory cachexia (Figure 2). Main indicator of the stages is the percentage of the weight loss as it independently predicts mortality of the cachectic patients. Pathways by which the weight loss occurs are increased energy expenditure, decreased appetite and malfunctions of the metabolic mechanisms. (Petruzzelli & Wagner 2016). The first stage, precachexia, is featured with mild cachectic symptoms e.g. moderate weight loss (<5 %), anorexia and abnormal glucose tolerance (Penet & Bhujwalla 2015). In addition, metabolic alternation e.g. elevated lipolysis level via activity of protein kinase A (PKA) is observed and overall energy production starts to rely more heavily on fat oxidation. (Murphy et al. 2012; Kliewer et al. 2015). Colon-26 carcinoma (C26) tumor bearing mice show increased muscle fatigability and lower grip strength resulting a decreased quality of life. Development towards cachexia requires greater weight loss (>5 %) but also other symptoms

are observed e.g. skeletal muscle atrophy. (Murphy et al. 2012). In refractory cachexia, the weight loss cannot be controlled due to the high catabolic rate nor does the nutritional support reverse the weight loss. Significantly decreased treatment tolerance with severe metabolic dysfunctions shortens the life expectance of the refractory state patient to less than three months. (Penet & Bhujwalla 2015). Another set point is loss of the original body weight by 30 %, after which death is very likely (Vaughan et al. 2013). Symptoms of decreased mobility, VO_2, locomotor speed and peak muscle strength in C26 bearing mice emphasize the detrimental effects of cancer cachexia on skeletal muscle (Murphy et al. 2012).

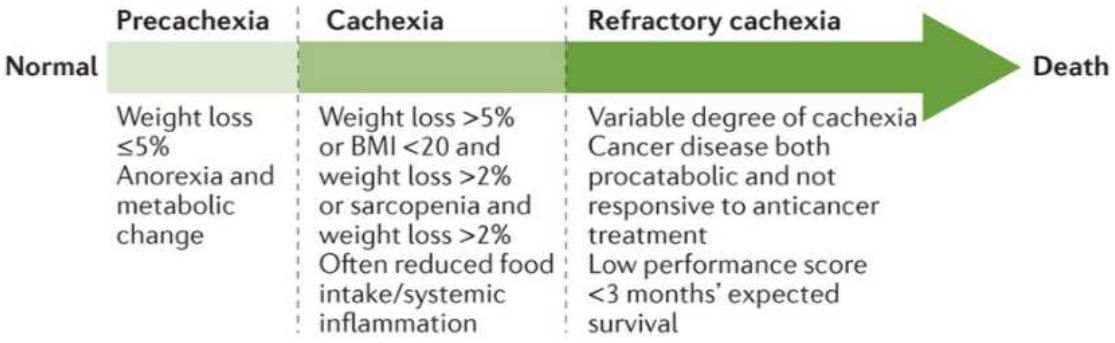

FIGURE 2. Progression of cancer cachexia and diagnostic tools to evaluate disease severity. Precachexia is featured with less than 5 % weight loss and as disease proceeds to cachexia weight loss is greater than 5 %. Body mass index (BMI) <20 correlates with the body weight reduction and lowered appetite. At the stage of refractory cachexia patients are too weak to tolerate various anti-cancer treatments and due to altered metabolism their life expectancy is significantly decreased. (Anandavadivelan & Lagergren 2016).

2.2 Hypermetabolism and thermogenesis in cancer cachexia

Tumors activate interscapular brown adipose tissue (BAT) thermogenesis in an unknown manner and increase heat production which is thought to lead to hypermetabolism (Kir et al. 2014; Petruzzelli et al. 2014). Mitochondrial uncoupling proteins (UCPs) in brown and beige adipocytes have been presented to be explanation of hypermetabolism in cancer cachexia as when the expression of uncoupling protein 1 (UCP1) is elevated in the mitochondria of BAT, a switch from the adenosine triphosphate (ATP) synthesis towards heat release occurs. (Fearon et al. 2012). Hypermetabolism increases oxygen consumption and decreases

respiratory exchange ratio (RER) even though physical activity is not increased nor food intake is decreased. This suggests that fat is preferred as an energy source thus leading to increased energy consumption, negative energy balance and weight loss in cachectic patients. (Kir et al. 2014).

Energy balance of the body is composed of the gained calories from food and the lost calories by energy consumption. Total energy expenditure (TEE) can be divided to three parts; resting energy expenditure (REE), diet-induced energy expenditure (DEE) and activity-induced energy expenditure (AEE). One additional type of energy expenditure is non-exercise activity thermogenesis (NEAT) which includes all the other energy requiring tasks except sleeping, eating and sports-like activity (Levine 2002). Cancer patients have higher REE at certain body weight than healthy people (REE > 110% of predicted), in part due to the high energy demands of the tumor (Fearon et al. 2012). It is also possible that tumorkines, referring here to the cytokines produced by the tumor, such as interleukins and tumor necrosis factor α (TNF-α), could activate BAT thermogenesis. This could increase the energy expenditure observed in cancer cachexia. (Tsoli et al. 2016). In cachectic C26 tumor bearing mice comparable results were obtained; resting energy expenditure (REE) increased, total energy expenditure (TEE) decreased and carbohydrate oxidation decreased while fat oxidation increased. (Murphy et al. 2012).

Weight losing cancer patients have also increased gluconeogenesis and glycogenolysis rates which are related to increased energy expenditure. This phenomenon is most likely caused by a combination of abnormal mitochondrial function, overexpression of hexokinase II and oncogenes (e.g. Ras and Akt), loss of tumor suppressor activity (e.g. p53) and hypoxic surroundings of the tumor. (Fearon et al. 2012). Other possible way how cancer cachexia affects glucose and amino acid metabolism is that it promotes oxidation of branched-chain amino acids, e.g. leucine, from skeletal muscle to become a substrate for gluconeogenesis thus resulting increased energy expenditure. (Vaughan et al. 2013). Increased adrenergic activity and systemic inflammation are also related to hypermetabolic state of the cancer patients. (Fearon et al. 2012). Futile cycles also increase energy expenditure in cachexia, e.g. the Cori cycle between the tumor and the liver. In this pathway, lactic acid from the tumor is converted to pyruvate and further to glucose in the liver. Then the newly formed glucose is transported back to the tumor where again lactate is produced and the high energy demanding cycle continues. (Vaughan et al. 2013). As well, other pathways between anabolic and catabolic reactions seem to cause hypermetabolism in cancer cachexia. (Argilés et al. 2015). Impaired

glucose metabolism and insulin resistance are also observed in many cancer patients (Tsoli & Robertson 2013).

Tumors consume considerable amounts of glucose as they produce ATP by glycolysis which is not as efficient way to produce energy as is oxidative phosphorylation. Uptake of glucose by colon carcinoma tumor is 30-fold and the release of lactate is 43-fold when compared to peripheral tissues emphasizing the role of the tumor as a high energy and high glucose consumer. (Tisdale 1997). In contrast, mRNA levels of the glucose transporter type 4 (GLUT4) in WAT is decreased in cachectic mice in combination with decreased insulin levels. This suggests that that overall glucose facilitation into adipose tissue decreases in cancer cachexia (Bing & Trayhurn 2009).

3 LIPID METABOLISM OF THE ADIPOSE TISSUE IN CANCER CACHEXIA

The roles of the white and brown adipose tissue in energy homeostasis are varied as white adipocytes store energy as triglycerides (TGs) while brown adipocytes use large extent of TGs to heat production. White and brown adipocytes are originated from the different precursors and their mitochondrial physiology differs which might explain their different primary functions. (Bournat & Brown 2010; Tsoli et al. 2016). Lipid metabolism in the adipose tissue is thought to be altered in cancer cachexia as lipolysis increases and lipogenesis is impaired e.g. due to the WAT browning phenomenon in which white adipocytes are turned to UCP1 expressing beige cells with thermogenic properties (Tsoli et al. 2016). With other so called browning markers, such as peroxisome proliferator-activated receptor-γ coactivator 1α (PGC-1α), peroxisome proliferator-activated receptor γ (PPARγ) and parathyroid hormone related protein (PTHrP), UCP1 switches the energy production to heat release in mitochondria of the brown and beige adipocyte. This promotes adipose tissue wasting and weight loss observed in cancer cachexia. (Lo & Sun 2013; Ebadi & Mazurak 2014).

3.1 Differences between white and brown adipose tissue

White adipose tissue. The main function of the white adipocytes is to take care of the energy homeostasis and store energy as TGs into intracellular lipid droplets when there are excessive amount of nutrients available. When energy is needed, WAT will release non-esterified fatty acids (NEFAs) to provide fuel for the ATP production. (Bournat & Brown 2010). WAT also acts as a secretory organ releasing adipokines, controlling appetite, inflammation, and insulin sensitivity (Ebadi & Mazurak 2014). White adipocytes are morphologically monolocular referring to their one large lipid droplet and they are sizewise usually larger than brown adipocytes. White adipocytes are a heterogeneous and versatile group of cells as they can be converted into beige adipocytes with higher mitochondria content due to multiple physiological and pathophysiological stimuli. They can also expand and shrink depending on the nutritional status. (Jeanson et al. 2015). Alternations in e.g. hormone secretion, insulin resistance, hyperglucagonemia and proinflammatory cytokine release as a result of the tumor

growth changes the function and metabolism of the white adipocytes (Argilés et al. 2015). Normal function of the WAT is essential for healthy life as it is involved e.g. in lipid and cholesterol metabolism, function of the immune system and reproduction (Tsoli et al. 2016).

Brown adipose tissue. Brown adipocytes are highly oxidative and insulin sensitive multilocular cells with numerous small intracellular lipid droplets (Orava et al. 2011; Jeanson et al 2015). They contain multiple mitochondria that give BAT its characteristic brown color and great heat production ability because of the expression of the fatty acid (FA) oxidation enzymes and components of the respiratory chain (Bournat & Brown 2010; Cohen & Spiegelman 2016). Expression level of the UCP1 in the mitochondria of brown adipocytes is high and therefore it uncouples the normal ATPase function in the inner mitochondrial membrane leading to proton leakage and heat production (Figure 3). This is referred as non-shivering thermogenesis and it is important for the regulation of the normal body temperature. (Giralt & Villarroya 2013; Jeanson et al. 2015). Sympathetic nervous system (SNS) is one of the main regulators of BAT activity via β-adrenergic stimulation (Sanchez-Delgado et al. 2015).

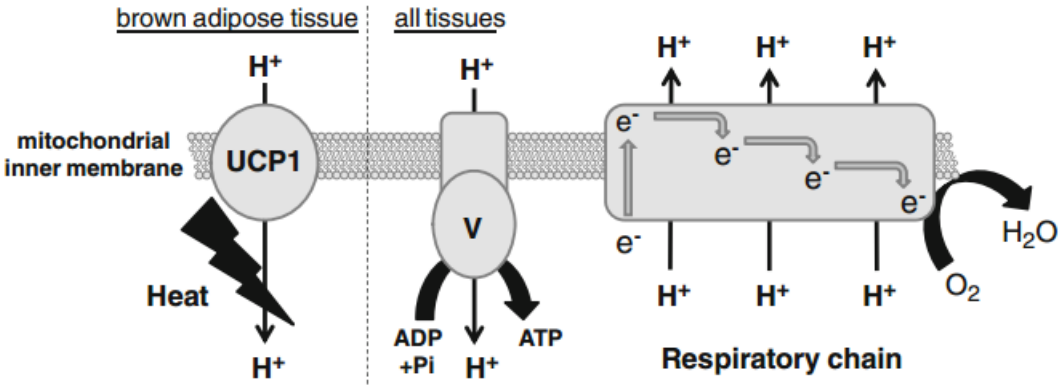

FIGURE 3. Uncoupling of the ATPase activity in BAT. UCP1 impairs mitochondrial proton gradient formation thus decreasing the activity of ATPase (Complex V). The switch from ATP production to heat release avails weight loss in cachexia. (Klingersporn & Fromme 2012, p 44).

Demands for the vascularization and blood perfusion in BAT are high due to the high nutrient and oxygen delivery requirements to maintain heat production when thermogenesis is activated (Orava et al. 2011; Betz & Enerbäck 2015). During prolonged thermogenic activity, e.g. in cancer cachexia, the increased blood perfusion in BAT is important for FA and glucose

uptake from the circulation as the TG content of BAT is insufficient to maintain long heat production. (Sanchez-Delgado et al. 2015). For adequate glucose uptake, BAT has more GLUT4 than WAT which also emphasizes the differences of the two tissues (Orava et al. 2011).

At a pleasant temperature, di- and triphosphate nucleotides inhibit the function of the UCP1 in BAT and thus only small amount of heat is produced. In the cold conditions, SNS is activated and noradrenaline is released to promote lipolysis and thermogenesis in brown and beige adipocytes. Also, increased lipolysis itself is a stimulus to promote BAT thermogenesis via increased number of FAs available from WAT and circulation for heat release (Tsoli et al. 2016). Another effect of noradrenaline in response to prolonged cold exposure is mitochondriogenesis. This increases thermogenesis in BAT as higher number of mitochondria enables greater oxidation of FAs. (Jeanson et al. 2015). In addition to cold activation of BAT, glucose activates brown adipocytes as well but differently than cold. Insulin-mediated glucose uptake increases without elevated blood perfusion as after cold exposure activation of BAT thermogenesis is dependent on increased perfusion. (Orava et al. 2011).

3.2 Adipose tissue wasting

Cancer cachexia wastes both skeletal muscle and adipose tissue. The latter is lost faster in part due to altered food intake and hormonal circulation (Fouladiun et al. 2005). Several pathways have been suggested to be the cause the adipose tissue loss during cancer cachexia, e.g. enhanced lipolytic actions, decreased activity of lipoprotein lipase (LPL), lower level of *de novo* lipogenesis and browning of the white adipocytes with increased level of inflammatory actions. (Henriques et al. 2017). Most likely the progressively increasing catabolic activity via lipolysis is the major pathway of the adipose tissue atrophy during the development of cancer cachexia (Bing & Trayhurn 2009: Henriques et al. 2017). Besides, lipolysis also impairs lipogenesis and dysfunctions in lipid-storage mechanisms can also affect adipose tissue atrophy. (Bing & Trayhurn 2009). Indeed, at cachectic state both in murine models and human studies have shown adipocyte atrophy, fibrosis and infiltration of the inflammatory cells into adipose tissue. These factors can cause impairments in normal WAT function and decrease the ability of the tissue to e.g. maintain lipid-derived hormone metabolism as human studies have shown hypogonadism in male cancer patients with advanced disease. (Strasser et

al. 2006; Henriques et al. 2017). In addition, the structure of the adipocytes alters in cancer cachexia as adipocytes become smaller but the interstitial space expands. As the conformation of the adipocyte cell membrane goes through remodeling accompanied with increased number of mitochondria in the cytosol of the adipocyte referring to WAT browning, alternation of the primary function of the tissue occurs. (Bing & Trayhurn 2009).

Mechanism of lipolysis is straight forward; one triglyceride is hydrolyzed to one glycerol and three FAs by different lipases. (Fearon et al. 2012). Adipose triglyceride lipase (ATGL), the first enzyme of the catabolic pathway in lipolysis, breaks down the triacylglycerol to one FA and diacylglycerol (DAG). In the next step, hormone sensitive lipase (HSL) releases the second FA as it hydrolyses the formed DAG to monoacylglycerol (MAG) which is further processed to glycerol and a third FA by MAG lipase (MAGL). (Tsoli et al. 2016). ATGL has a dominant role in the initiation of lipolysis and it acts as a rate limiting enzyme in the breakdown of the triglycerides. Sympathetic stimulus and noradrenaline act via β-adrenoreceptors to activate PKA to initiate lipolysis via ATGL. Also, AMP-activated protein kinase (AMPK) activates ATGL to increase the rate of lipid deposit breakdown. (Petruzzelli et al. 2014). It is shown that both C26 and Walker 256 tumor-bearing rats have increased AMPK activity at the early stage of cachexia thus suggesting impaired *de novo* lipogenesis rate as the uptake and/or intracellular handling ability of the FAs has decreased. (Henriques et al. 2017).

Loss of the WAT in cachectic mice was prevented by using an AMPK-stabilizing peptide (ACIP) which blocks the interaction between Cell death-inducing DFFA-like effector A (CIDEA) and AMPK. In fact, as ACIP encoding sequence via adeno-associated virus (AAV) was injected to the inguinal WAT (iWAT) of the C26 tumor bearing mice, iWAT weight was on average 30 % greater than control mice with empty AAV. As well, lipid droplets of ACIP C26 tumor-bearing mice were larger than in control mice with empty AAV. AMPK is activated by low ATP levels, a state observed in cancer cachexia e.g. due to high rates of energy consuming futile cycles. Previously mentioned role of the UCP1 and BAT thermogenesis in adipose tissue wasting has recently been questioned as UCP1 knockout did not show prevention of adipose tissue loss in cancer. This suggests that WAT browning at least through UCP1 may not be an important mediator of cachexia. In addition, UCP1 mediated WAT thermogenesis due to WAT browning has also been under critical consideration as mRNA and protein levels of UCP1 are lower than in BAT and thus possibly

do not have large relevance. Due to these new results of UCP1 actions in cancer cachexia and adipose tissue wasting, the role of WAT thermogenesis should maybe be rethought. (Rohm et al. 2016).

If the ATGL and HSL are inhibited during cancer cachexia, the release of FAs and glycerol will decrease by 85 % at least from gonadal WAT in mice (Petruzzelli et al. 2014). In another study, ATGL and HSL knockout mice with Lewis lung carcinoma (LLC) or B16 melanoma were used and the inhibition of ATGL protected the mice from adipose tissue and muscle loss. FA release from WAT decreased in both lipase knockout groups when compared with control group. Inhibition of HSL showed similar but less significant results as the ATGL knockout model. (Das et al. 2011). At this point one must take into consideration that most likely this kind of lipase blockade can possibly alter the energy homeostasis regulation of the body as also other tissues than just adipose tissue have lipases e.g. liver and skeletal muscle can break down triglycerides. (Doolittle et al 1987; Badin et al. 2011).

Interleukin-6 (IL-6) and TNF-α are released from the tumor and they may increase lipolysis and fat depletion in cancer patients (Tsoli & Robertson 2013). In cachectic patients with advanced colo-rectal cancer, WAT is lost most rapidly approximately within the three months prior to death when monitored by retrospective computed tomography. The amount of FAs in the plasma can rise as much as 5-fold due to loss of adipose deposits in cancer cachexia (Tsoli et al. 2014). The amount of glycerol also increases because of the increased lipolysis and IL-6 (Tsoli & Robertson 2013). Cachectic patients have higher turnover rate of the released FAs and glycerol when compared with the cancer patients without cachectic symptoms suggesting enhanced utilization of fat (Bing & Trayhurn 2009). Both inflammatory cytokines that either inhibit lipogenesis or promote lipolysis as well as β-adrenergic activation have a promoting effect on the WAT wasting rate in cancer cachexia (Fearon et al. 2012; Petruzzelli et al. 2014). More precisely, lipolysis is more important to wasting of WAT than inhibition of the lipogenesis (Tsoli & Robertson 2013; Petruzzelli & Wagner 2016).

In cancer cachexia, at least part of the adipose tissue wasting has been suggested to be a result of the UCP1 mediated BAT thermogenesis and WAT browning. As activity of BAT mitochondria increases via multiple pathways, e.g. tumorkines, more TGs from WAT are broken down and released to the circulation to refill energy needs of BAT. (Petruzzelli et al.

2014). Figure 4 shows the pathways and mediators of lipolysis and adipose tissue atrophy in cancer cachexia.

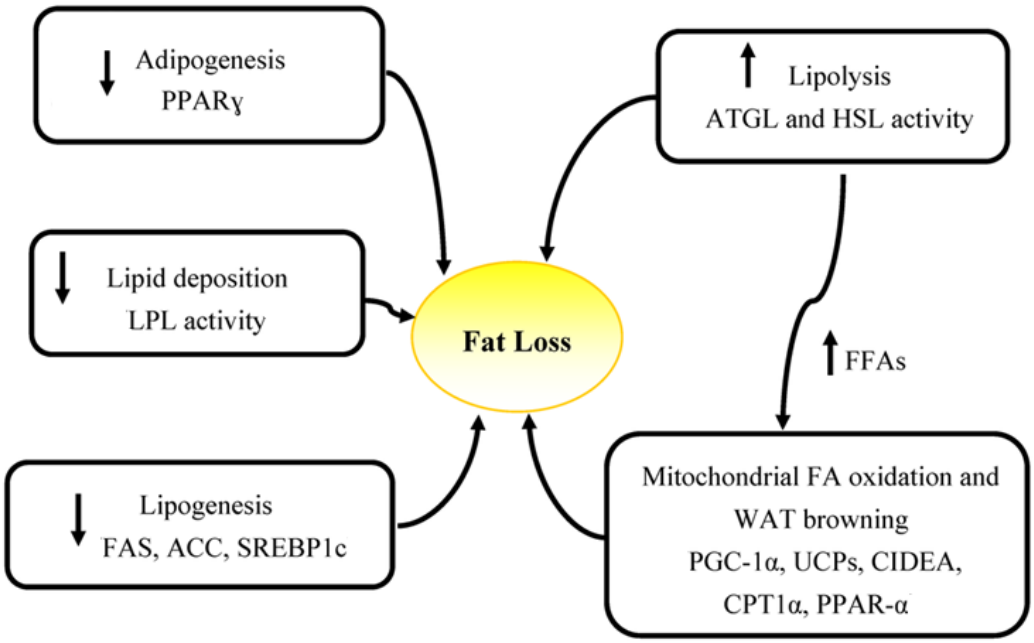

FIGURE 4. Regulatory pathways and mediators of the WAT wasting during cancer cachexia. In cancer cachexia, formation of the new TG stores is downregulated due to increased lipolysis. As well, impaired lipogenesis via altered function of fatty acid synthase (FAS), acetyl-CoA carboxylase (ACC) and sterol regulatory element binding protein-1c (SREBP1c) decrease TG formation. Thus, greater amount of FFAs are released into the circulation for further processing e.g. for β-oxidation or heat production in the BAT. Cell death-inducing DFFA-like effector A (CIDEA), carnitine palmitoyltransferase 1α (CPT1α). (Modified, Ebadi & Mazurak 2014).

3.3 White adipose tissue browning

During WAT browning phenomenon, white adipocytes are turned into “beige” or “brite” (brown in white) cells thus gaining features of the brown adipocytes. There are multiple mechanisms that can activate WAT browning including long cold exposure, cancer related tumorkines, high redox pressure, stress, irisin and β3-adrenergic agonist (Lo & Sun 2013; Petruzzelli et al. 2014; Jeanson et al. 2015). From different adipose tissue deposits, UCP1 expression and browning of WAT are most plausible to develop into iWAT or subcutaneous WAT (scWAT) than to visceral or epididymal WAT (vWAT and eWAT, respectively) (Lo & Sun 2013; Jeanson et al. 2015). Brown and beige adipocytes have similarities in their

metabolism as they have more mitochondria and lipid droplets than white adipocytes and they both express UCP1 (Sidossis & Kajimura 2015). UCP1 is upregulated by IL-6 which is a pro-inflammatory cytokine. (Penet & Bhujwalla 2015). Also, other markers are related to WAT browning e.g. PGC-1α, PPRARγ, PTHrP, CIDEA and PR domain containing 16 (PRDM16). (Petruzzelli et al. 2014; Jeanson et al. 2015; Tsoli et al. 2016).

Despite the similarities of the brown and beige adipocytes, they differ in origin. In Figure 5 is shown how brown adipocytes are originated from the dermomyotomes meaning that they are more closely related to skeletal muscle development than to WAT development. (Sidossis & Kajimura 2015). The common precursor of brown adipocytes and myocytes expresses myogenic factor 5 (Myf5) which is a myogenic lineage marker and makes the metabolic profiles of BAT and skeletal muscle very similar (Bournat & Brown 2010; Giralt & Villarroya 2013). Similarly to white adipocytes, beige adipocytes are originated from mesodermes and they are related to WAT formation (Sidossis & Kajimura 2015). These beige cells that undergo functional change during WAT browning are Myf5 negative which highlights their different primary origin when compared to 'classical brown adipocytes' (Myf5 positives). Brown adipose tissue is developed substantially earlier than white adipose tissue as the formation of BAT begins during fetal life. Development of WAT starts after birth when energy storage is required. (Giralt & Villarroya 2013).

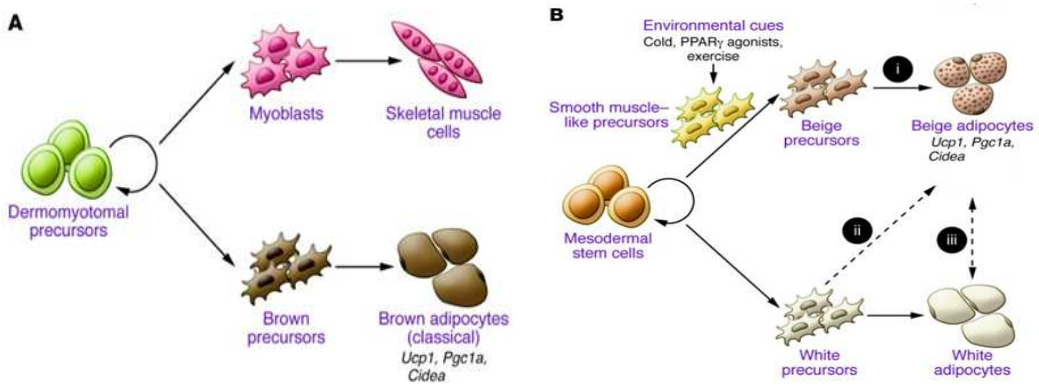

FIGURE 5. Origins of the adipocytes. (A) Brown adipocytes differ from beige and white adipocytes (B) as they are originated from dermomyotomal precursors instead of mesodermal stem cells. Developmental differences may explain functional differences between adipose tissue types. Production of UCP1, PGC-1α and CIDEA by brown and after WAT browning also by beige adipocytes is an indicator of thermogenesis in the mitochondria. (Modified, Sidossis & Kajimura 2015).

One theory of the WAT browning in cancer cachexia is associated with elevated intracellular reduction-oxidation (redox) pressure in white adipocytes via high plasma lactate concentration as a response to non-specific stress. When lactate is transported into WAT by monocarboxylate transporters (MCTs) it is converted to pyruvate by lactate dehydrogenase B (LDHB). This increases the $NADH/NAD^+$ ratio as well as intracellular redox pressure and this elevated redox state promotes WAT browning via UCP1. After respiratory chain function is uncoupled, oxidation of NADH increases in the mitochondria of WAT and this lowers the $NADH/NAD^+$ ratio towards normal. In this sense, WAT browning is thought to be an alternative way to decrease high redox pressure observed in white adipocytes during cancer cachexia. Additionally, oxidative stress and high redox state can also be thought to be regulators of the UCP1 expression in adipocytes. WAT browning could also be an adaptive thermoregulatory response to maintain normal body temperature during cancer cachexia. (Jeanson et al. 2015). Alternatively, exogenous factors can also activate browning of WAT, more about this in chapter 3.4.

Ways to identify different adipocyte types are insufficient as now the phenotype of WAT is described as a lack of markers of the beige or brown adipocytes. This is extremely problematic for e.g. at the beginning of WAT browning when part of the cells are already turned into beige but still whole tissue is characterized as WAT (Jeanson et al. 2015). Insulin sensitivity of the brown and beige adipocytes is higher than the white adipocytes thus enabling them to use glucose as a source of energy at a higher rate (Argilés et al. 2015). Therefore, WAT browning phenomenon has interested medical companies from the obesity and type 2 diabetes mellitus point of view. Medicine development to obesity related diseases is under intense research nowadays and dissipation of energy as heat by BAT is one of the hot topics. This emphasizes how in some cases browning of WAT can be beneficial and in others it can be devastating. (Chondronikola et al. 2014; Tsuchida 2014).

3.4 Regulators of the white adipose tissue browning

There are multiple markers involved in WAT browning (Lo & Sun 2013). Some of the most important regulators are PGC-1α, PRDM16, PPRARγ, IL-6, type II iodothyronine deiodinase (DIO2) and PTHrP (Kir et al. 2014; Petruzzelli et al. 2014; Betz & Enerbäck 2015; Jeanson et al. 2015). Also, other pathways that cause WAT browning are found, e.g. β-adrenergic

pathway and systemic inflammation but they are not presented here in detail (Petruzzelli & Wagner 2016). It is worth to mention and remember that all the above mentioned browning regulators have also other functions in multiple other pathways in cellular metabolism so they are not only specific to brown adipocytes, UCP1 expression or the white adipose tissue browning (Jeanson et al. 2015). This highlights the complexity of the metabolic pathways related to cancer cachexia and the difficulty to develop treatment for the disease.

PGC-1α. PGC-1α promotes expression of the uncoupling proteins in adipocytes thus controlling mitochondriogenesis, oxidative phosphorylation and thermogenesis via UCP1 (Lo & Sun 2013; Tsoli et al. 2016). In addition, PGC-1α is thought to promote the release of irisin protein which also may have a positive effect on WAT browning (Argilés et al. 2015). Function of the PGC-1α in WAT browning is also to be a coactivator of PPARγ to increase lipolysis and FA oxidation in cachectic patients even during increased caloric intake (Lo & Sun 2013; Ebadi & Mazurak 2014).

PRDM16. At first it was thought that PRDM16 is only expressed in BAT but now it is shown to be present in scWAT as well (Seale et al. 2011; Tsoli et al. 2016). In fact, PRDM16 has a vital role in promotion of the WAT browning as it guides the cell fate of an adipocyte towards a beige phenotype and it downregulates white adipocyte genes (Cao et al. 2011; Giralt & Villarroya 2013; Lo & Sun 2013). Expression of the brown-fat like genes e.g. PPARγ and PGC-1α is promoted by PRDM16 as it acts as their co-regulator. (Giralt & Villarroya 2013). In dermomyotomal precursors, PRDM16 is a co-regulator of the selection whether the cell will become a skeletal muscle cell or a brown adipocyte as in the absence of PRDM16 the cells will become skeletal muscle cells. If PRDM16 is expressed in brown adipocyte it will upregulate UCP1 and CIDEA expression thus promoting thermogenesis and adipose tissue wasting in cancer cachexia. (Tsoli et al. 2016).

PPARγ. PPARγ is a vital transcription factor in all adipocytes and it greatly promotes UCP1 expression at transcriptional level in adipose tissue (Lo & Sun 2013; Jeanson et al. 2015). Similarly to PRDM16, PPARγ upregulates BAT related genes while downregulating WAT related genes (Lo & Sun 2013). Another role of PPARγ in the regulation of the lipid metabolism occurs via gene expression as PPARγ controls the genes involved in FA synthesis, oxidation, transport, uptake and release (Kershaw et al. 2007). PPARγ forms a WAT browning regulatory complex with PRDM16 and to activate the PPARγ, sirtuin 1

(SIRT1) deacetylation is required (Figure 6). As the complex is activated, WAT browning occurs and expression of the brown-fat-like genes is upregulated and white-fat-like genes are downregulated in white adipocytes. (Lo & Sun 2013). If the function of the PPARγ is abnormal in BAT, brown adipocytes have monolocular lipid droplets and thus they look like a white adipocyte accompanied with decreased UCP1 expression when exposed to cold environment. This emphasizes the importance of PPARγ as a key mediator of the normal BAT function. (Jeanson et al. 2015). PPARγ promotes lipolysis also by regulating levels of the ATGL via PPAR responsive element as there is a positive correlation between PPARγ and ATGL mRNA and protein expression in adipose tissue (Kershaw et al. 2007; Das & Hoefler 2013).

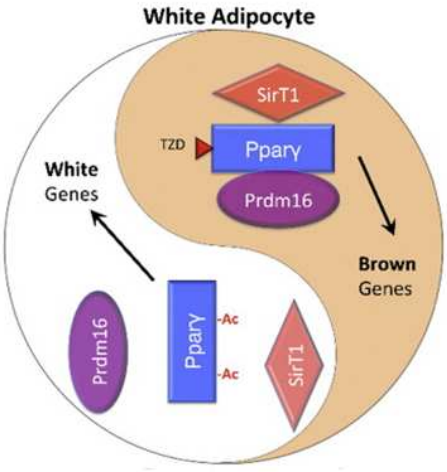

FIGURE 6. PPARγ-PRDM16 complex promotes WAT browning in cancer cachexia. PPARγ is deacetylated via Sirtuin1 (Sirt1) prior to PPARγ-PRDM16 complex activation. As a result, the complex promotes the expression of the brown adipocyte-like genes thus inducing WAT browning and thermogenesis in cancer cachexia. (Qiang et al. 2012).

IL-6. Skeletal muscle, adipose tissue and tumor(s) among other organs produce IL-6 so it can be defined either as a myokine, adipokine or tumorkine, respectively (Tsoli et al. 2016). IL-6 drives the systemic inflammation during the development of cancer cachexia and it promotes acute phase response of which the liver is responsible (Fearon et al. 2012). In cancer cachexia, the tumor derived IL-6 release is continuous and there no longer exist normal feedback mechanisms to control it. This most likely alters the normal IL-6 function towards a mediator of tissue wasting in cancer cachexia. IL-6 has its own metabolic pathways in each above-

mentioned organ but at the same time it also acts as a link between them to maintain energy homeostasis of the body. The networks in which IL-6 takes part are both catabolic (e.g. β-adrenergic pathway) and anabolic (e.g. insulin signaling pathway) so this emphasizes the importance of IL-6 as an energy balance regulator also in cancer cachexia. (Tsoli et al. 2016). Total blocking of IL-6 release by short hairpin RNA (shRNA) in C26 tumor-bearing mice prevented total body weight loss. In addition, inhibition of the UCP1 expression in scWAT was simultaneously observed thus inhibiting WAT browning. (Petruzzelli et al. 2014). Increased amount of IL-6 in the circulation has a positive correlation with weight loss and reduced survival rate (Fearon et al. 2012, Petruzzelli et al. 2014). By inhibiting IL-6, cachectic symptoms like anemia and anorexia can be treated but this will not prevent the loss of skeletal muscle. Side effects of the IL-6 inhibition are severe and that is why anti-IL-6 therapy is not recommended for patients with early stage of cancer cachexia. (Petruzzelli et al. 2014).

DIO2. DIO2 is closely related to energy homeostasis as it converts tyroxine (T4) to triiodothyronine (T3). Thyroid hormones have the ability to make BAT more sensitive for adrenergic stimulation by SNS which activates the cold induced BAT thermogenesis. (Christoffolete et al. 2004; Betz & Enerbäck 2015). DIO2 knockout mouse model has shown an activation of the cyclic adenosine monophosphate (cAMP) responsive genes thus suggesting impaired thermogenesis in these mice (Christoffolete et al. 2004).

PTHrP. Parathyroid hormone (PTH) and its related protein PTHrP are structurally quite similar regulators of the calcium homeostasis. The main difference between these two is that PTHrP acts as a para- or autocrine manner instead of PTH which is a classical hormone. (Schlüter 1999). Abnormal regulation of PTHrP is related to skeletal metastasis development which is why PTHrP could be considered as an ideal target for cancer treatment. (Kremer et al. 2011, pp 145). Many tumors express PTHrP and it can directly activate thermogenic gene expression in adipose tissues as it upregulates UCP1, DIO2 and PGC1-α mRNA production. PTHrP and PTH both increase oxygen consumption and thus they act as a regulators of the cellular respiration. (Kir et al. 2014). Hypercalcemia is a commonly observed metabolic dysfunction in cancer patients and this phenomenon is related to increased PTHrP activity (Porporato 2016). By blocking PTHrP, adipose tissue browning and loss of the skeletal muscle and adipose tissue mass have been blocked in mice without affecting the tumor size. (Penet & Bhujwalla 2015). Also, the inhibition of PTHrP decreased the expression of UCP1 and PGC1α which could lead to WAT browning inhibition (Tsoli et al. 2016). Other features observed improving the cachectic symptoms were lowered oxygen consumption and

thermogenesis combined with increased overall activity that increased the quality of life. This suggests that inhibition of PTHrP reduces WAT browning and adipose tissue wasting. (Kir et al. 2014).

Summary. As can be seen, multiple regulators are involved in the adipose tissue metabolism during cancer cachexia. It is good to notice that these browning mediators do not act alone. Most likely their combined actions to WAT browning are greater together than the effect of a single mediator alone. (Tsoli et al. 2016). The WAT browning as a phenomenon in cancer has also received conflicting results (Rohm et al. 2016) and thus more research is needed. Figure 7 summarizes the factors related to WAT browning, mediators of thermogenesis in BAT and other features closely in related to pathways and regulation of cancer cachexia.

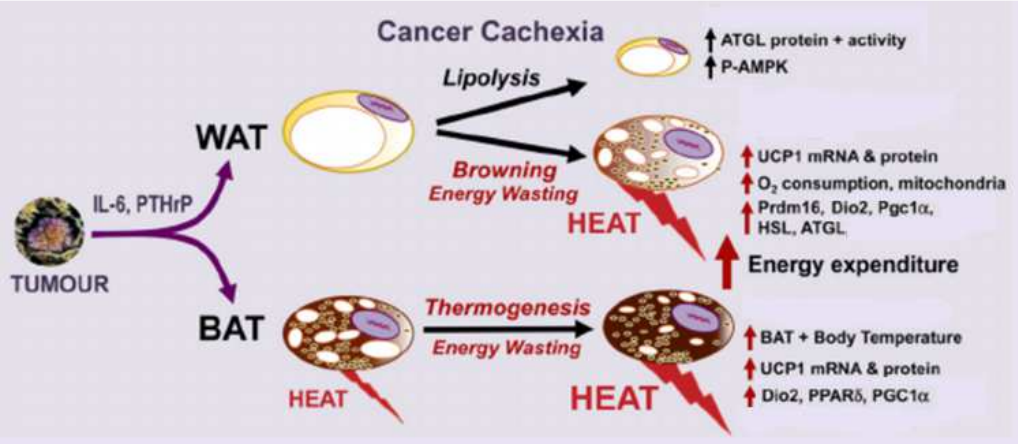

FIGURE 7. Summary of the mediators in the WAT browning and BAT thermogenesis during the development of the cancer cachexia. Tumor derived IL-6 and PTHrP alter the adipose tissue metabolism by promoting lipolysis and heat release. Adipose tissue atrophy observed in cancer cachexia is caused by the increased lipolysis in WAT via ATGL, HSL and AMPK activity. In addition, heat release from BAT also avails loss of adipose deposits. Multiple factors cause WAT browning as expression of UCP1, PRDM16, type II iodothyronine deiodinase (DIO2) and PGC-1α in beige adipocytes increases. In BAT, PPARγ, DIO2 and PGC-1α cause heat release similarly as in beige adipocytes. (Modified, Tsoli et al. 2016).

4 LIPID METABOLISM OF THE SKELETAL MUSCLE IN CANCER CACHEXIA

Increased lipolysis in adipose tissue during cancer cachexia alters also the metabolism of the skeletal muscle. As increased number of FAs are released from the white adipocytes into the circulation, uptake of these lipid products increases in the skeletal muscle. (Petruzzelli & Wagner 2016). This leads to a formation of larger intramyocellular lipid droplets of cachectic patients if the usage of FAs does not increase. Indeed, cachectic gastrointestinal cancer patients have shown an increase in lipid storage into skeletal muscle in comparison to weight-stable cancer patients. As the skeletal muscle lipid content increases, it may be a signal of an impaired mitochondrial FA utilization and/or β-oxidation which may be related to reduced survival rate. (Turner et al. 2007; Stephens et al. 2011). Increased FA uptake also activates synthesis of ceramides and decreases activity of the mammalian target of rapamycin (mTOR) pathway thus inhibiting the protein synthesis rate (Petruzzelli & Wagner 2016).

4.1 Lipid accumulation into skeletal muscle in cancer cachexia

Lipid droplets in the skeletal muscle have an important role as energy storage for the mitochondrial FA oxidation e.g. during prolonged exercise or increased energy demand. They are commonly located next to the mitochondria to allow fast energy transportation. (Stephens et al. 2011). Infiltration of FAs into skeletal muscle during cachexia may alter the function of the tissue as it may reduce muscle strength (Lipina & Hundal 2016). In addition, function of the skeletal muscle may already be impaired as muscle fatigue and weakness are observed due to muscle atrophy. Ubiquitin-dependent proteasome pathway is shown to be upregulated in cachexia and that causes degradation of the contractile proteins. Accumulation of FAs into the skeletal muscle disturbs the normal function of the contractile system and downregulates protein synthesis possibly by inhibiting mTOR pathway. Expression of atrophy-related genes, atrogens, e.g. Atrogin1 and muscle RING-finger protein1 (MuRF1) is increased because of the increased lipid influx into skeletal muscle. (Petruzzelli & Wagner 2016).

Human studies have shown that the size of the intramyocellular lipid droplets positively correlates with severity and progression state of cachexia (Stephens et al. 2011). Similarly,

murine models have shown that intramyocellular lipid droplets become larger and their number increases during the development of the cancer cachexia. (Julienne et al 2012; Das & Hoefler 2013). Mice with LLC induced cancer cachexia has been shown to have higher TG concentrations in the gastrocnemius muscle when compared to the control mice. This is possibly due to the alternations of the lipid metabolism as well as increased lipolysis in the adipose tissue. (Das & Hoefler 2013). It is suggested by Tsoli and Robertson (2013) that the increase of the intramyocellular lipid droplet content is caused by impaired instead of increased lipolysis in cachectic mice. Indeed, same is suggested by Petruzzelli & Wagner (2016) as they report that murine models of cachexia have shown decreased FA uptake and TG synthesis in WAT. Difference in human cachexia is that it is also related with enhanced lipolysis but accompanied with unaltered lipogenesis rate. (Petruzzelli & Wanger 2016).

Inhibition of mTOR pathway and protein synthesis in cancer cachexia may be in part mediated by increased FA uptake into to skeletal muscle (Petruzzelli & Wagner 2016). Therefore, utilization of lipids increases in the mitochondria. By inhibiting both mTOR complexes, mammalian target of rapamycin complex 1 and 2 (mTORC1 and mTORC2), lipid-utilization is observed but if only the mTORC1 is blocked the same observation is not seen. This suggests that the mTORC2 regulates also the lipid metabolism as it does glucose metabolism in the skeletal muscle via Perilipin 3 (PLIN3). Overexpression of PLIN3 in the skeletal muscle leads to an increase of the intracellular TG content. Importance of the mTORC2 is shown by using knockout mice lacking the activity of mTORC2. These knockout mice had lower RER meaning that they were more reliant on lipid metabolism as an energy source than the wildtype mice. One of the other main findings was that mTORC2 knockouts had similar body weight as the wildtypes but their body composition differed significantly; knockouts had lower skeletal muscle mass and approximately 30 % higher fat mass when compared to wildtypes. Increased fat mass was observed also in the skeletal muscle as the intracellular triglyceride content increased 65 % in the mTORC2 knockout mice. (Kleinert et al. 2016).

4.2 Fatty acids and lipid derivatives as regulators of the skeletal muscle mass and function

As lipolysis increases in cancer cachexia due to WAT atrophy, increased number of FAs are released into the circulation. When infiltrated into skeletal muscle, FAs and their lipid derived metabolites can change the normal function and mass of the target tissue. These lipid molecules can alter muscle cell growth, proliferation as well as their differentiation thus leading to abnormal muscle function. (Lipina & Hundal 2016).

Saturated and unsaturated FAs have opposite functions in relation to muscle mass regulation. One of the most common circulating saturated FAs, palmitate (C16:0), is shown to upregulate expression of atrogens, leading to increase of forkhead box O3 (FOXO3) nuclear localization when administered to muscle cells. Palmitate also enables the accumulation of toxic lipid intermediates such as ceramide thus inhibiting protein synthesis and PKB/Akt pathway. Promotion of muscle atrophy also occurs when palmitate is given to C2C12 cells as after this treatment myotube diameter has decreased. Skeletal muscle nutrient status can be endangered as amino acid availability may decrease due to the actions of ceramide as it downregulates the expression of the sodium-dependent neutral amino acid transporter 2 (SNAT2). (Lipina & Hundval 2016). In addition, ceramide downregulates phospholipase D (PLD) which is an mTOR activator and it is shown that inhibition of ceramide synthesis could preserve the size of the myocyte in cachexia and other muscle wasting promoting diseases (De Larichaudy et al. 2012). In contrast, unsaturated FAs like docosahexaenoic acid (DHA) do not seem to promote muscle atrophy. On the contrary, when C26 adenocarcinoma tumor-bearing mice were fed with linoleic acid, an omega-6 polyunsaturated fatty acid (PUFA), gastrocnemius muscle mass was not reduced and expression of muscle TNF-α receptor was decreased. Observed data suggests that the usage of PUFAs may inhibit muscle atrophy and suppress TNF-α actions in the skeletal muscle. In fact, human studies have shown that omega-3 PUFAs e.g. eicosapentaenoic acid (EPA) and omega-6 PUFA DHA may be related to promotion of increased lean muscle mass and improved muscle strength at least in the long term use. (Mantovani et al. 2006; Ma et al. 2015; Smith et al. 2015). As well, unsaturated FAs may counter the effects of saturated FAs as e.g. PUFAs in gastrocnemius muscle can reduce the amount of TNF-α and Toll-like receptor 4 (TLR4) that promote pro-inflammatory actions.

TLR4 activation is shown to promote protein catabolism in C2C12 cells as it enhances the actions of both ubiquitin-proteasome system and autophagy-lysosome pathway. (Lipina & Hundval 2016).

4.3 Crosstalk between adipose tissue and skeletal muscle

Endocrine activity of the WAT is high as white adipocytes produce many adipokines e.g. leptin, TNF-α and IL-6 that can have auto-, para-, and endocrine functions (Kim & Moustaid-Moussa 2000; Das & Hoefler 2013). WAT produces also endocrine and nuclear hormones, cytokines and catecholamines and it controls appetite and nutrient metabolism (Das & Hoefler 2013; Tsoli & Robertson 2013). In the same way skeletal muscle acts as an endocrine organ by secreting myokines with para- and endocrine functions as well as other factors such as hormones, cytokines and FAs. (Das & Hoefler 2013). These mediators continue passing their effects also during cancer cachexia (Fearon et al. 2012). High levels of FAs, ceramides and DAG from WAT can have lipotoxic effects in the skeletal muscle as there is a possibility that they cause lipid overload due to dysfunctions in lipogenesis, lipolysis and/or lipid oxidation. Therefore, these FAs may induce insulin resistance and impair muscle development. Same is true for the products of the skeletal muscle; they can alter WAT metabolism and mass of the target tissue. (Das & Hoefler 2013).

Understanding the crosstalk between the adipose tissue and skeletal muscle (Figure 8) as well as other organs linked to cancer cachexia is an important part of the development of diagnostics tools and therapeutic interventions. As WAT is wasted may be wasted prior to skeletal muscle in cancer cachexia, blocking the adipose tissue weight loss could potentially slow down the loss of skeletal muscle. (Das & Hoefler 2013).

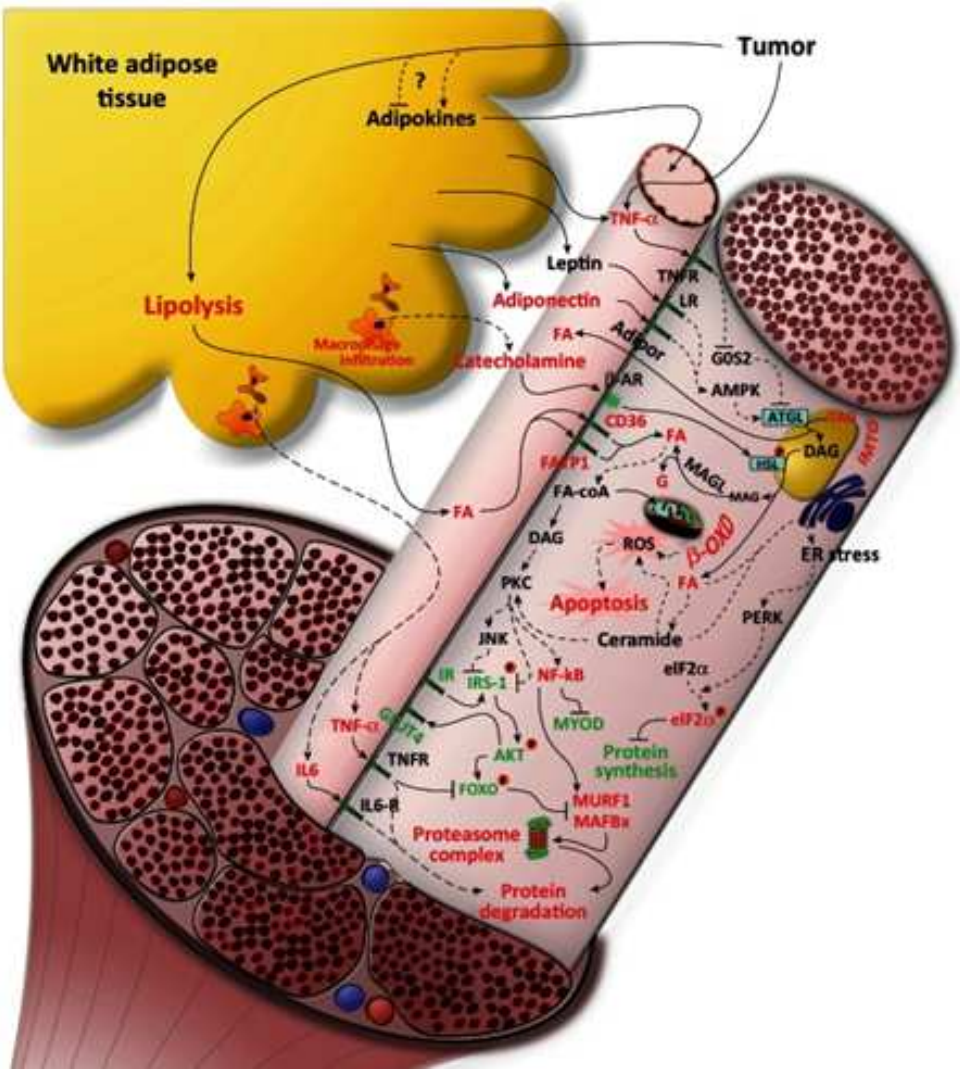

FIGURE 8. Crosstalk pathways between WAT, tumor and skeletal muscle in cancer cachexia. Adipokines from WAT and myokines from skeletal muscle have auto-, para- or endocrine functions that affect other organs related to cachexia. (Das & Hoefler 2013).

5 ACTIVINS AND MYOSTATIN IN CANCER CACHEXIA

Activin A (ActA) and myostatin are important regulators of the skeletal muscle mass and growth. They bind to an activin receptors type 2A and 2B (ACVR2A/B) on cell membrane and mediate their functions signaling via smad family member type 2 (Smad2) and FOXO3a to promote quiescence of the skeletal muscle stem cells and protein degradation via ubiquitin-proteasome pathway. By blocking the ACVR2B receptor with its soluble form (sACVR2B-Fc), further muscle wasting can be prevented and loss of skeletal muscle can be reversed. (Zhou et al. 2010).

5.1 Activin A and myostatin mediating skeletal muscle wasting

ActA and myostatin are ligands of the transforming growth factor β (TGF-β) family that act via ACVR2A and 2B receptors. This pathway has a key role in regulating the skeletal muscle growth, overall muscle mass and skeletal muscle satellite cell quiescence via ACVR2B-Smad pathway. (Zhou et al. 2010). ACVR2B pathway is involved in the skeletal muscle atrophy as it promotes ubiquitin-proteasome mediated myofibrillar protein degradation and decreases Akt/mTOR related protein synthesis. (Tisdale 2010; Chen et al. 2014; Loumaye et al. 2015). As ActA or myostatin binds to ACVR2B receptor on the cell membrane, activity of Smad2/3 and FOXO3a increases. Phosphorylation of Smad2/3 decreases the muscle cells growth ability by various ways such as by inhibiting the satellite cells activity. Another result is that activated Smad2/3 dephosphorylates FOXO3a to activate MuRF1 and Atrogin1 expression in the nucleus, leading to higher ubiquitination rate of contractile proteins, especially myosin (Figure 9). Ubiquitination is a signal to protein degradation via proteasome system and this leads to skeletal muscle wasting in cancer cachexia. (Zhou et al. 2010). Thus, ACVR2B pathway has been suggested to be one of the most important signaling pathways both in the development and progression of the cancer cachexia (Chen et al. 2014).

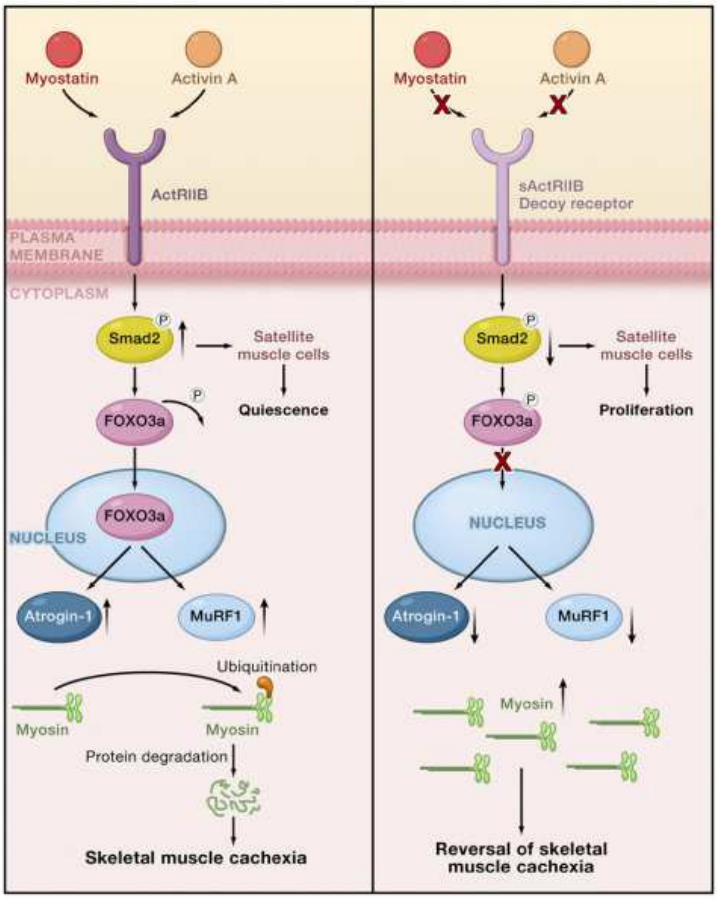

FIGURE 9. Pathway of the ubiquitin-proteasome mediated muscle degradation via ActA and myostatin in cancer cachexia (on the left) acting via ACVR2B. Activation of the Smad2 and FOXO3a keeps the satellite cells quiescent and promotes ubiquitin ligases Atrogin-1 and MuRF1 expression thus wasting the skeletal muscle. Blockade of ActA and myostatin activity e.g. by sACVR2B-Fc (on the right) decreases the activity of smad2 and FOXO3a thus reversing the skeletal muscle wasting due to inhibited protein degradation and promoting a synthesis of new skeletal muscle by activating satellite cells. (Tisdale 2010).

Concentration of the circulating ActA increases e.g. in acute inflammation, renal failure and some cancers thus promoting muscle atrophy and adipose tissue wasting even without a tumor. Correlation between increased ActA and decreased strength of the skeletal muscle in cachectic patients demonstrates the importance of the ActA as a disturbing mediator of the normal muscle function. This loss of strength is mainly due to alternations in the skeletal muscle function via ActA as well as increased intracellular lipid accumulation into skeletal muscle cells. Similarly to ActA, increased expression of the negative muscle growth regulator

myostatin may also lead to wasting of the skeletal muscle in cancer cachexia. (Loumaye et al. 2015; Lee et al. 2016). After birth, myostatin is expressed predominantly in the skeletal muscle but it is also detected in the circulation. It is still under debate if the circulating myostatin has endocrine activity or could it enter the active protein pool in the skeletal muscle and thus regulate muscle mass. To the date, it seems that myostatin has both para- and endocrine functions. Locally in the muscle produced myostatin determines the mass of that specific muscle referring to paracrine activity. Endocrine activity of myostatin is shown by a mosaic mice model in which myostatin production is inhibited in the posterior muscles but not in the anterior muscles. The mass of the posterior muscles was significantly decreased due to circulating myostatin expressed in the anterior muscles. (Lee et al. 2016).

Myostatin inhibits muscle growth by decreasing Akt/mTOR pathway activity and protein synthesis in the skeletal muscle (Tsuchida 2014). By using specific antibodies, e.g. follistatin, function of myostatin can be blocked leading to increased muscle mass and decreased fat accumulation in mice (Rebbapragada et al. 2003; Tsuchida 2014). In myostatin knockout mice the same is observed as hypertrophy and hyperplasia is detected (Tsuchida 2014). Human response is identical as inhibition or a loss-of-function mutation in myostatin protein increases the number and size of myofibrils in children and muscle mass in the adults (Hatakeyama et al. 2016).

5.2 Blocking of the ACVR2B pathway

It is suggested that in the development of cancer cachexia, ActA could be the key regulator over the classical cytokines due to mostly ineffective treatment of patients with anti-TNF-α and/or anti-IL-6 antibodies when compared to more effective method by using sACVR2B-Fc to block ActA (Zhou et al. 2010; Loumaye et al. 2015). Indeed, as shown in Figure 10, muscle atrophy decreases and the survival rate increases by blocking the ActA and myostatin pathways in murine models (Loumaye et al. 2015). It is also shown that muscle wasting can be fully reversed in mice (Chen et al. 2014). This treatment was effective even without tumor growth inhibitors accompanied with unaltered levels of adipose tissue wasting and pro-inflammatory cytokine production. The rate of protein degradation via the ubiquitin-proteasome system decreases by the ACVR2B blockade while the growth of muscle stem cells has increases. Timing of the first sACVR2B-Fc dose for cachectic C26 mice can be in even in the advanced state of cachexia as the sACVR2B-Fc is able to reverse skeletal muscle

atrophy in mice with more than 10 % weight loss thus increasing the survival rate tremendously. (Zhou et al. 2010).

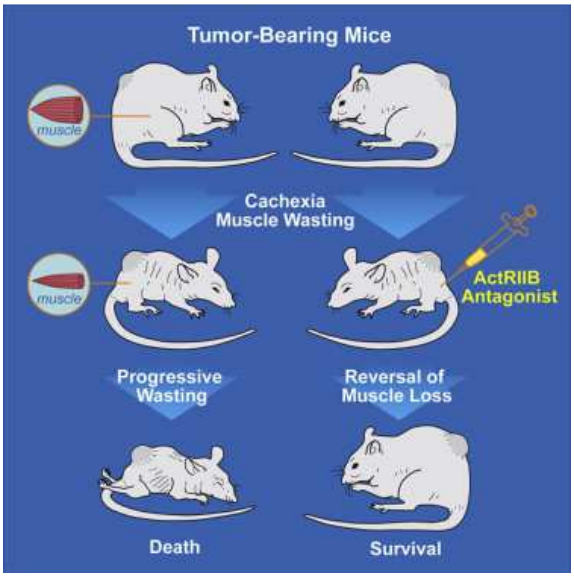

FIGURE 10. Blockade of ACVR2B pathway can reverse and prevent the loss of skeletal muscle in murine models by inhibiting the ubiquitin-proteasome system. The treatment does not affect the tumor growth and still the life expectancy has increased significantly. (Zhou et al. 2010).

Treatment of the cachectic and healthy mice with sACVR2B-Fc show comparable results. Blocking of the ACVR2B pathway by sACVR2B-Fc enhances protein synthesis in the skeletal muscle already one or two days after the beginning of the treatment thus promoting muscle growth in healthy mice. (Hulmi et al. 2013). Similarly, cachectic mice have shown to increase skeletal muscle mass with sACVR2B-Fc treatment (Zhou et al. 2010). As well, sACVR2B-Fc treatment has been shown to prevent chemotherapy-induced muscle atrophy via restoration of muscle protein synthesis levels (Nissinen et al. 2016).

Contradictorily, sACVR2B-Fc treatment can cause WAT browning that promotes function of the mitochondria. This increases thermogenesis, lipogenesis, energy expenditure and weight loss of the cancer patients. This also raises a question whether it is more important to preserve the skeletal muscle mass than adipose tissue mass in the treatment of cachexia as by saving and increasing lean mass survival rate of cancer patients has increased even when adipose tissue is lost. (Tsuchida 2014).

6 RESEARCH QUESTIONS AND HYPOTHESES

Lack of effective cure for cancer cachexia in humans makes the research of the topic very vital. Currently, the cause of cachexia is unknown and traditional methods (e.g. nutritional support) have not been able to deliver the wanted outcome it is important to seek the answer from multiple tissues and tissue interactions. As the loss of the white adipose tissue is clearly shown to occur in cancer cachexia in multiple murine and human cancer models (Das et al. 2011; Petruzzelli et al. 2014) it makes the tissue interesting from the treatment point of view. Weight loss in cancer cachexia is an undesirable symptom and if adipose tissue atrophy could be prevented it would be interesting to see how that affects metabolism at whole body level and does it have effect on cancer survival.

6.1 Research questions

1) Does WAT browning occur in experimental C26 and does the blocking of the ACVR2B pathway by the sACVR2B-Fc change the gene expression and function of the white adipose tissue. Changes of WAT browning markers are observed at mRNA and protein level by RT-qPCR and Western blot.
2) Does lipid accumulation into skeletal muscle occur in experimental C26 and does the blocking of ACVR2B pathway by the sACVR2B-Fc alter lipid metabolism in the skeletal muscle. Changes in lipid metabolism in the skeletal muscle are observed by measuring the triacylglycerol content of the gastrocnemius muscle.

6.2 Hypotheses

1. WAT browning occurs in cancer cachexia as many different browning regulators e.g. tumorkines and myokines are secreted into circulation and taken up by WAT. These regulators switch the gene expression of white adipocytes towards genes of the brown adipocytes thus making them beige and giving them thermogenic ability. Inhibition of the ACVR2B pathway activates WAT browning and oxidative capacity of the WAT mitochondria thus increasing thermogenesis, energy expenditure and weight/adipose tissue loss in cancer cachexia.

Arguments: Adipose tissue metabolism during cancer cachexia has been studied in multiple rodent models e.g. C26, LCC, MAC16, Walker 256, LLC and B16 (Das et al. 2011; Tsoli et al. 2015) and browning of WAT has been shown in many earlier studies including murine models with LCC, C26 and B16 cancers (Kir et al. 2014; Petruzzelli et al. 2014). On the other hand, by using the same cancer models e.g. C26, WAT browning was not observed by others (Kliewer et al. 2015). A switch from the white adipocyte phenotype towards the beige adipocytes expressing UCP1 occurs due to many regulators e.g. PGC-1α, PPARγ and PRDM16 (Lo & Sun 2013; Pertuzzelli et al. 2014). There are some controversial results about the role of the UCP1 mediated adipose tissue thermogenesis and weight loss during cancer cachexia as UCP1 knockout did not show prevention of adipose tissue loss in cancer (Rohm et al. 2016). Blockade of the ACVR2B pathway increases skeletal muscle protein synthesis and decreases adipose tissue mass (Zhou et al. 2010; Tsuchida 2014). Use of the sACVR2B-Fc in C26 tumor-bearing mice prevented the loss of the skeletal muscle but simultaneously adipose tissue was wasted thus suggesting non-protective role of this treatment on adipose tissue (Zhou et al. 2010). In addition, administration of the sACVR2B-Fc can increase expression of the UCP1 and PGC-1α significantly thus suggesting enhanced thermogenic ability of beige cells due to WAT browning at least in high-fat diet consuming mice. This might be a result of inhibiting binding of sACVR2B-Fc to ligands of the thermogenic repressors. (Koncarevic et al. 2012). As well, blockade of ACVR2B pathway promotes mitochondrial functions and thermogenesis in BAT thus enabling the FA usage to heat production. (Fournier et al. 2012).

2. Lipid accumulation into the skeletal muscle occurs in cancer cachexia as a consequence of increased lipolysis and FA release from the WAT. This increases intramyocellular lipid droplet content in the skeletal muscle thus impairing FA utilization and β-oxidation leading the impaired muscle function. (Stephens et al. 2011). mTOR pathway is impaired due to increased FA uptake leading to inhibited protein synthesis. (Petruzzelli & Wagner 2016). Overall, the sACVR2B-Fc treatment is known to decrease adipose tissue mass (Koncarevic et al. 2012), but less is known how it affects intramuscular lipid droplet content.

Arguments: Previous studies have shown the detrimental effect of lipid accumulation into skeletal muscle and how it affects muscle strength and function (Lipina & Hundal 2016; Petruzzelli & Wagner 2016). During muscle wasting, the ubiquitin-proteasome system

requires a lot of ATP to breakdown proteins. This and other high energy consuming pathways of cancer cachexia, e.g. futile Cori cycle due to lactate production, are a great burden to mitochondria. To deal with this high ATP demand, mitochondria must decrease the efficiency which is related with energy wasting as all the oxygen is not used to ATP production. If efficiency decrease of mitochondria does occur in the skeletal muscle, it could increase energy expenditure significantly, even 15-30 % of the basic metabolic rate. As well, the decreased oxidative capacity of the muscle is related to accumulation of intramyocellular lipid droplets and insulin resistance. (Van Herpen & Schrauwen-Hinderling 2008; Julienne et al. 2012).

On the other hand, total lipid accumulation into the skeletal muscle in the early state of cachexia has not been observed in other studies (Kliewer et al. 2015). On the whole-body level sACVR2B-Fc treatment does not prevent adipose tissue loss, in fact blockade of myosin activity can even decreases body fat mass, but it prevents lipid accumulation into liver preventing liver steatosis at least in high-fat dieting mice (Koncarevic et al. 2012). At the moment, little is known and more research is needed about the effect of sACVR2B-Fc treatment on skeletal muscle lipid accumulation.

7 MATERIALS AND METHODS

7.1 Animals

In the study BALB/c (BALB/cAnNCrl) male mice aged 5-6 weeks from Charles River Laboratories (Germany) were used. They were housed in the groups of three in standard conditions (temperature 22°C, 12-h dark, 12-h light cycle). Free access to food pellets (R36; 4% fat, 55.7% carbohydrate, 18.5% protein, 3 kcal/g, Labfor, Stockholm Sweden) and tap water was provided during the entire experiments.

C26 was selected to be the cancer type as these C26 bearing mice develop severe cachexia with significant decrease in body, muscle and adipose tissue mass in a short period of time as well as they show increases in inflammation markers and ubiquitin ligases. Due to skeletal muscle fiber atrophy this model also shows decrease in muscle strength and physical activity accompanied with fast muscle fatigue. All the described symptoms are observed also in human cancers so this murine model is close to clinical conditions of cancer patients. (De Larichaudy et al. 2012; Murphy et al. 2012).

7.2 Ethics statement

The treatment of the animals was in strict accordance with the European Convention for the protection of vertebrate animals used for experimental and other scientific purposes. The protocol was approved by the national animal experiment board, permit number: ESAVI/10137/04.10.07/2014.

7.3 Experimental design

The aim of the study was to determine if the sACVR2B-Fc administration to C26 bearing mice until the cancer or until death would decrease adipose tissue atrophy, affect WAT browning and prevent TG accumulation into the skeletal muscle. Duration of the study was 11 days and the mice were randomized into one of the three groups (n = 9 in each): PBS with C26 (PBS + C26), sACVR2B-Fc before C26 injection (ACVR b) and continuous sACVR2B-

Fc (ACVR c). Additionally, healthy control group (n = 9) was included and they were injected with PBS (Figure 11). Five outlier mice from cancer groups (two from PBS + C26, two from C26 + ACVR b and one from C26 + ACVR c) did not grow a prober tumor so they had to be excluded from the statistical determinations resulting 7, 7 and 8 mice per group, respectively. From this onward if not mentioned otherwise number of the mice per group in figures is 7-8 as described above.

sACVR2B-Fc (5 mg/kg) or PBS was injected 100 µl intraperitoneally three times before C26 (or PBS for control) inoculation and three times after cancer cell transplant. Activity of the mice was measured with force plate at basal level (day -13, 13 days before C26 (or PBS) cell inoculation) and a second time one day before the end of the study (day 10, 10 days after C26 (or PBS) cell inoculation). Mice and the eaten food were weighted daily. None of the mice had to be euthanized prematurely. At day 11, after the mice were anesthetized by mixture of ketamine and xylazine (Ketaminol® and Rompun®, respectively), the heart puncture was taken and euthanization followed by cervical dislocation. Next, the tissue samples (GA (gastrocnemius), soleus, TA (tibialis anterior), tumor, and subcutaneous and epididymal WAT (white adipose tissue)) were collected, weighted and stored into liquid nitrogen as quickly as possible. Tibia length was measured to normalize skeletal muscle weights. Muscle weights reported in this thesis are an average of the weights of the right and left leg. In Figure 11 is shown a schematic presentation of the study design.

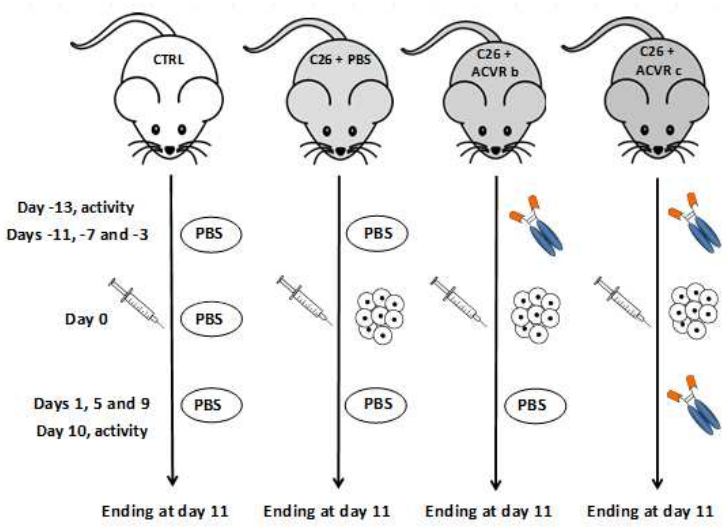

FIGURE 11. Study design. Mice were randomized to one of the groups; control (CTRL), PBS with C26 (PBS + C26), sACVR2B-Fc before C26 (ACVR b) and continuous sACVR2B-Fc treatment (ACVR c). Before C26 cell (or PBS to CTRL) inoculation, mice were injected with PBS (CTRL and C26 + PBS) or sACVR2B-Fc (C26 + ACVR b and C26 + ACVR c). After this, PBS was injected to CTRL, C26 + PBS and C26 + ACVR b groups. sACVR2B-Fc treatment was continued for the C26 + ACVR c group. In the beginning of the study n = 9 per group.

7.4 Force plate measurements

Activity of the mice was determined by 24 h force plate measurement at their own home gage. At day -13, 13 days prior to cancer cell (or PBS) inoculation, gage was placed on the force plate surface and all the movement above the threshold (background was removed) was summed together from 24 h period and divided by the mass of the mouse. By these means the activity index data was collected. Measurement was repeated at day 10, 10 days after cancer cell inoculation.

7.5 sACVR2B-Fc production

In this study, a recombinant fusion protein that was produced and purified *in house* in the University of Helsinki by O. Ritvos and A. Pasternack as described by Hulmi et al. (2013) was used. Shortly, ectodomain of human ACVR2B was added to the human IgG1 FC domain to produce required fusion protein sACVR2B-Fc. Firstly, PCR was used to amplify the human ectodomain. The sequences of the primers used in PCR of sACVR2B were the

following; 5′-GGACTAGTAACATGACGGCGCCCTGG-3′ and 5′-CCAGATCTGCGGTGGGGGCTGTCGG-3′. Secondly, the human IgG Fc domain with a COOH-terminal His6 tag was amplified and the primer sequences were; 5′-GCAGATCTAATCGAAGGTCGTGGTGATCCCAAATCTTGTGAC-3′ and 5′-TCCCTGTCTCCGGGTAAACACCATCACCATCACCATTGAGCGGCCGCTT-3′ as previously shown by Hulmi et al. (2013). Chinese hamster ovary cells were used to produce the final protein product. His-tag was used to collection of the recombinant protein from Ni^{2+}-loaded HiTrap Chelating column and purity of the eluate was determined to be > 90 % by silver-stained SDS-PAGE.

7.6 Triacylglycerol extraction from gastrocnemius muscle

Gastrocnemius muscle samples were pulverized in liquid nitrogen and further homogenized into chloroform-methanol (2:1) in relationship of 30 mg sample in 4 ml of buffer added by weight as previously described by Bruce et al. (2007). Organic and non-organic phases were separated by adding 0.9 % (wt/vol) NaCl as demonstrated by Bruce et al. (2007) and the lower organic phase was evaporated by vacuum evaporator. Absolute ethanol was used to dissolve the dried triacylglycerol and the concentration was measured by Triglycerides kit (#981786, Thermo Scientific) with KoneLab measuring device (Thermo Scientific, Vantaa, Finland).

7.7 RNA extraction and RT-qPCR

RNA extraction. Total RNA was extracted from the pulverized scWAT samples with QIAzol Lysis Reagent (1023537, QIAGEN) by the protocol of the RNeasy Plus Universal Mini Kit (73404, QIAGEN,). Concentration and purity of the extracted RNA was determined spectrophotometrically by NanoDrop as absorbance at 260/280 nm wavelengths was measured. Mean A260/A280 in CTRL group was 2.09, in C26 + PBS group 2.11, in C26 + ACVR b 2.09 and in C26 + ACVR c 2.1. To convert RNA to cDNA for RT-qPCR analysis, iScript™ Adv cDNA kit for RT-qPCR (#172-5038, Bio-Rad Laboratories) was used by the protocol of the manufacturer.

RT-qPCR. Real-time quantitative polymerase chain reaction (RT-qPCR) was used to determine the expression of UCP1, DIO2, PRDM16, IL-6, PGC-1α1 and housekeeping genes TATA-box binding protein (TBP), 18S ribosomal RNA (Rn18S), glyceraldehyde 3-phosphate dehydrogenase (GAPDH), ribosomal phosphoprotein P0 (RPLP0, a.k.a 36B4) (Table 1). The thermocycling protocol of the RT-qPCR consisted three stages; firstly, at high temperature DNA strands were separated as they denaturate due to the heat. As the temperature was decreased, the primers bounded to the template and second temperature rise will begin the elongation in which new strand is synthesized by DNA polymerase. One whole cycle of the three steps will double the copied DNA number. (Garibyan & Avashia 2013). In this study SYBR green, a double stranded DNA-binding dye, was used to detect the products. (Real-time PCR handbook, 12). All the preparation steps for the RT-qPCR were conducted in the laminar to minimize the possibility of contaminations. Firstly, primers, samples and reagents were melted on ice and SYBR green was protected from light. Samples were diluted 1:10 so that the total concentration was 8.5 ng/ul. Master mixes of the genes with BioRad ready-to-use primers consisted 10 µl of iQ™ SYBR® Green Supermix (#170-8882, Bio-Rad Laboratories), 1µl of primer (both 5' and 3' primers included) and 7µl RNase free water per one reaction. Master mixes of TBP, IL-6 and PGC-1α1 consisted 10 µl iQ SYBR Supermix, 1µl 5´ primer, 1µl 3´ primer and 6µl RNase free water per one reaction. These latter self-designed primers were diluted 1:10 from the stock. After pipetting 18 µl of the master mix to the 96 well plate, 2 µl (17 ng) of the sample was added making the total volume of one reaction to be 20 µl. To seal the plate, microseal 'C' film was used and plate was centrifuged 1000 rpm for 1 minute. For the UCP1, PRDM16 and DIO2 the temperature cycles were 2 minutes at + 95 ºC, 45 cycles of 5 seconds at + 95 ºC to denaturate and 30 seconds at + 60 ºC to anneal, elongate and detection. For IL-6, PGC-1α1, TBP, GAPDH and 36B4 the temperatures cycles were 10 minutes at + 95 ºC, 45 cycles of 10 seconds at + 95 ºC to denaturate, 30 seconds at + 60 ºC to anneal and + 72 ºC to extension and detection. After this amplification protocol, melting curve for each gene was determined by measuring the fluorescence between temperatures +65 ºC and +95 ºC with 0.5 ºC increments for every 5 seconds. CFX96 RealTime PCR Detection System (Bio-Rad Laboratories) was used to quantify the results. Efficiency corrected ΔCt method was used in the study to analyze the obtained data.

cDNA gel electrophoresis. TBP results were used to normalize the data as they were round the most stable between the groups of the tested housekeeping genes (Figure 12A, all data not

shown). In Figure 12B is shown the DNA gel electrophoresis of the TBP showing that the product from RT-qPCR is the same size (89 bp) as expected. To start with the DNA gel electrophoresis, the 3 % agarose gel was prepared as follows; 3.75 g of agarose was diluted to 0.5 X TBE buffer in the microwave and 2.5 µl of ethidium bromide was added and then the mixture was placed to set into the running device. Next, the cDNA samples were diluted 1:4 to water so that the total volume is 20 µl and 5 µl of sample loading buffer was added to the mixture. After mixing and spinning the samples 18 µl of the sample and 12 µl of TrackiIt 50 bp DNA ladder (#10488-043, Invitrogen) and was pipetted on the gel. 0.5 X TBE running buffer containing 16 µl of ethidium bromide was added to the running chamber and the samples were run at 100 V for 1 hour and 30 min for 150 V. Quantity One 4.6.3. - software (Bio-Rad Laboratories) was used for the detection.

TABLE 1. Primers used in the study. UCP1, PRDM16 and DIO2 were purchased from the BioRad® and the manufacturer does not provide the sequences of the transcripts.

Isoform/Transcript	**Forward 5´→ 3´**	**Reverse 5´→ 3´**
GAPDH	AACTTTGGCATTGTGGAAGG	GGATGCAGGGTGATGTTCT
IL-6	CTGATGCTGGTGACAACCAC	CAGAATTGCCATTGCACAAC
PGC-1α1	CATGTGCAGCCAAGACTCTG	ACACCACTTCAATCCACCCA
Rn18S	GCAATTATTCCCCATGAACG	GGCCTCACTAAACCATCCAA
TBP	GAAGCTGCGGTACAATTCCAG	CCCCTTGTACCCTTCACCAAT
36B4	GGCCCTGCACTCTCGCTTTC	TGCCAGGACGCGCTTGT

Isoform/Transcript	**Unique Assay ID, BioRad®**
DIO2	qMmuCID007430
UCP1	qMmuCID0005832
PRDM16	qMmuCID0010482

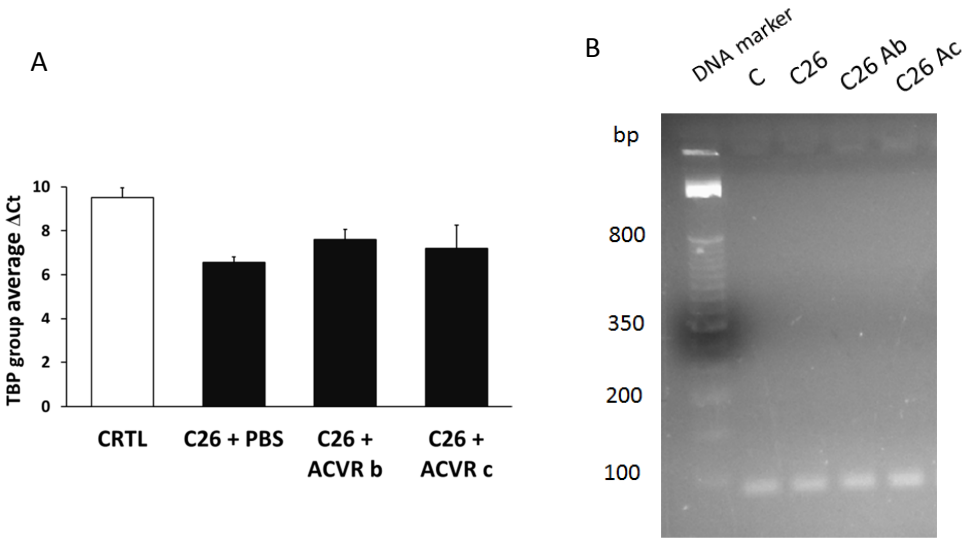

FIGURE 12. A) TBP group average ΔCt values expressed as ± SE shown no statistical differences between groups. B) The DNA gel electrophoresis of TBP showing that the synthetized product is the right size (89 bp). TrackIt 50 bp DNA ladder was used as a marker.

7.8 Citrate synthase activity

Activity of the citrate synthase (CS) was determined from the diluted scWAT homogenates (1:20) by using a specific kit (CS0720-1KT, Sigma-Aldrich) and an automated KoneLab measuring device (Thermo Scientific, Vantaa, Finland).

7.9 Western blot protein analysis

To prepare the scWAT and gastrocnemius samples ready for the Western blot analysis, they were first pulverized into liquid nitrogen and further homogenized as previously described by Hulmi et al. (2013) and diluted to ddH_20 so that protein content was 30 µg in 15 µl of a sample. To determine the protein quantity of the studied genes from scWAT and gastrocnemius muscle Western blot was conducted. Protein concentrations of the both tissues were determined by Pierce™ BCA Protein Assay Kit (#23225, Thermo Scientific) and KoneLab device. Genes of interest from scWAT were; ACC, p-ACC (Ser79), ATGL, Cyt *c*, p-HSL (Ser660), HSL, OXPHOS, PGC-1α, PLIN5, STAT3, p-STAT3 (Tyr705), UCP1 and

α-Tubulin. More details about the antibodies are shown in appendix. Control of the protein loading and transfer in the study was Ponceau S staining.

SDS-page. Protein samples were first diluted to the wanted concentration (30 µg of protein in 15 µl of sample) and mixed with 2 x Laemmli sample buffer (#161-0737, Bio-Rad Laboratories) with 5 % β-mercaptoethanol. In the next step, samples were shortly centrifuged and placed on the heat block (95 ºC) for 10 minutes, centrifuged shortly again and put on ice for 5 minutes. Prior to the sample loading (25 µl of each sample to the well), 6 µl of molecular marker (Precision Plus Protein™ Dual Color Standards, #161-0374, Bio-Rad Laboratories) was added to the gel (4-20 % Criterion™ TGX™ Precast Gels, #567-1094, Bio-Rad laboratories). Protein samples were separated by electrophoresis in electrophoresis running buffer (2.5 mM Tris Base, 19.2 mM glycine, 0.01 % SDS, ddH2O) with 270 V for 35 minutes at +4 ºC on ice. SDS denaturates the proteins thus making them negatively charged. This way proteins will move from the anode towards the cathode based on only their molecular weights.

Blotting. After SDS-page, proteins were blotted from the gel to the PVDF membrane (Amersham™ Hybond™ P 0.45 PVDF, GE Healthcare Life Sciences, 1060023). Before that the gel was placed into blotting buffer (2.5 mM Tris Base, 19.0 mM glycine, (pH adjusted to 8.3 with HCl), 10% methanol, ddH2O) for 30 minutes and in the mean while PVDF membrane was activated in the methanol for 10 seconds, next in the ddH2O for 2 minutes and finally in the blotting buffer for 15-20 minutes. Prior to building the blotting cassette, blotting buffer was added to wet the scotch-brite pads and blotting papers. Inside the cassette there were following components in this order; a scotch-brite pad, a blotting paper, the electrophoresis gel, the PVDF membrane, a blotting paper and a scotch-brite pad. Cassettes were placed into blotting chamber with magnetic stir and ice brick. Blotting buffer was added and blotting was conducted with 300 mA for 2.5 hours at +4 ºC on ice.

Ponceau S staining, blocking and primary antibodies. After blotting the membranes were stained in Ponceau S for 10 minutes, washed with ddH2O and imaged with Molecular Imager ChemiDoc XRS System (Bio-Rad) and Quantity One 4.6.3 –software (Bio-Rad). In the next step, membranes were cut so that only one protein of interest was on one strip and then the strips were blocked at room temperature for 2 hours in TBS + 0.1 % Tween-20 + 5 % non-fat milk in slow rocking. Meanwhile, primary antibodies (appendix 1) were prepared and then added to strips and they were incubated overnight at 4°C with gentle rocking.

Secondary antibodies and protein detection. The membranes were washed 4 x 5 minutes by TBS-Tween and incubated for 1 hour at room temperature with the secondary antibodies (appendix 1) with slow rocking. After 5 x 5 minutes of washing with TBS-Tween, the membranes were incubated with detection kit solution (SuperSignal West Femto Maximum Sensitivity Substrate, Pierce Protein Biology Products, #34096, Thermo Scientific) for 5 minutes and images were taken by 45 Molecular Imager ChemiDoc XRS System (Bio-Rad Laboratories) and Quantity One 4.6.3.-software (Bio-Rad Laboratories).

Stripping. Stripping was done for those membranes that had two proteins of interest and this way the first protein could be removed (p-STAT3 was stripped to detect STAT3 and PLIN5 was stripped to detect α-Tubulin). To do so, the strips were incubated in Western Blot stripping buffer (#21059, Thermo Scientific) for 30 minutes at the room temperature with rocking. The stripping solution was removed by rinsing the membranes 5 x with ddH_2O and 3 x 5 minutes of TBS-Tween. To avoid unspecific binding, blocking was conducted again. After this the strips were incubated with the new primary antibody as early described.

Quantification and notifications. Quantification and determination of relative quantities of the proteins of interest was done with Quantity One 4.6.3. - software (Bio-Rad Laboratories). To normalize the data mean of the wells of Ponceau S staining were used.

Note. OXPHOS differed in protocol from the other studied genes in SDS-page as the samples were heated for 7 minutes at 50 ºC instead of 10 minutes in 95 ºC. Same is true for PCG-1α as it was done in the same run as OXPHOS.

7.10 Data processing and statistical analyses

To analyze the data with statistical tests, IBM® SPSS® Statistics program version 24 was used (SPSS, Chicago, IL, USA). Data was tested for normality and equality of variances. Results were analyzed by Mann-Whitney U-test and corrected with Holm-Bonferroni except tissue weights were analyzed by one-way Anova LSD Post-hoc test corrected with Holm-Bonferroni. One other exception was CTRL vs. C26 + PBS group as it was analyzed with t-test. Pooled cancer effect was analyzed with Mann-Whitney U-test (CTRL vs. all C26 mice pooled). Pearson correlation was used to determine the relation of scWAT RNA and protein yield to scWAT mass per tibial length. Statistical significance was set at $p < 0.05$.

8 RESULTS

8.1 Body composition, physical activity and food consumption

In agreement with previous studies, the C26 alone (C26 + PBS) caused an expected decrease in the body weight, adipose tissue deposits and skeletal muscle mass when compared to the control group (Figures 13A, 15A-B and 16A-C, respectively). Cancer decreased the body weight of the C26 + PBS group when compared to the CTRL group ($p < 0.05$, Figure 13A) but the receptor blocker treatment reversed the skeletal muscle atrophy of both sACVR2B-Fc groups, statistically non-significantly in C26 + ACVR b group and significantly in C26 + ACVR c group ($p < 0.01$) when compared to C26 + PBS group (Figure 13A). Tumor size of the C26 bearing mice does not explain the changes in body weight as it did not differ between the cancer groups (Figure 13B).

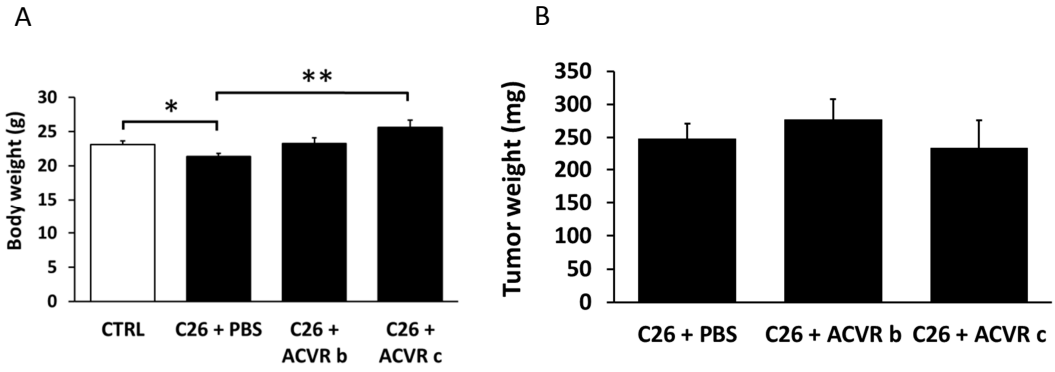

FIGURE 13. A) Body weight. * or ** depicts significant difference between the groups designated by lines ($p < 0.05$ and $p < 0.01$, respectively). B) Tumor weights do not show differences between cancer groups.

Three days (days 8-10) prior to the end of the study, there was decrease in eating in all C26 groups ($p < 0.05$) (Figure 14A). The group treated with sACVR2B-Fc only before to the C26 inoculation showed greater decrease in eating when compared to the continued sACVR2B-Fc treated group. There was also an expected negative cancer effect in the activity of the tumor-bearing mice when compared to control ($p < 0.01$) showing decreased physical activity in all cancer groups (Figure 14B).

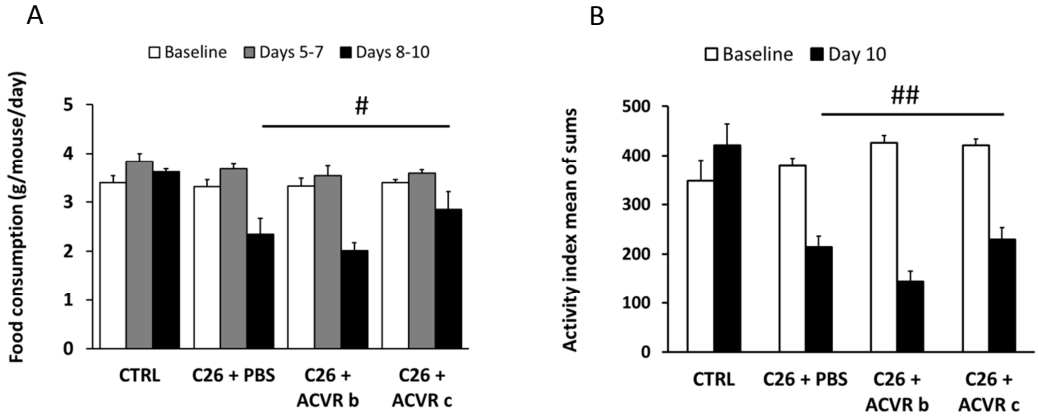

FIGURE 14. A) Food consumption at baseline (days -13 and -12), days 5-7 and days 8-10 after C26 inoculation. # with line depicts cancer effect at days 8-10, $p < 0.05$, n = 4 in CTRL group, 3 in others. B) Activity of the mice at baseline (day -13) and at day 10. ## depicts cancer effect at day 10, $p < 0.01$, n = 3 in C26 + PBS group, 2 in others.

The C26 has a significant cancer effect on adipose tissue mass as both scWAT and eWAT are decreased tremendously ($p < 0.001$) (Figure 15A and 15B, respectively). sACVR2B-Fc treatment did not have additional effect on the rate of adipose tissue atrophy, although continued sACVR2B-Fc treatment maintained the scWAT mass slightly better than if the treatment was ended after cancer cell injection ($p < 0.05$). The loss of the adipose tissue also decreased the amount of Perilipin 5 (PLIN5), an adipose cell surface protein which is related to homeostasis of lipogenesis and lipolysis by regulation of FA oxidation, storage and release (Dalen et al. 2007), showing a negative cancer effect ($p < 0.05$) (Figure 15C). Decrease in the skeletal muscle mass was prevented by the sACVR2B-Fc treatment and there was a statistically significant increase in the mass of the studied muscles over the PBS level (Figure 16A-C).

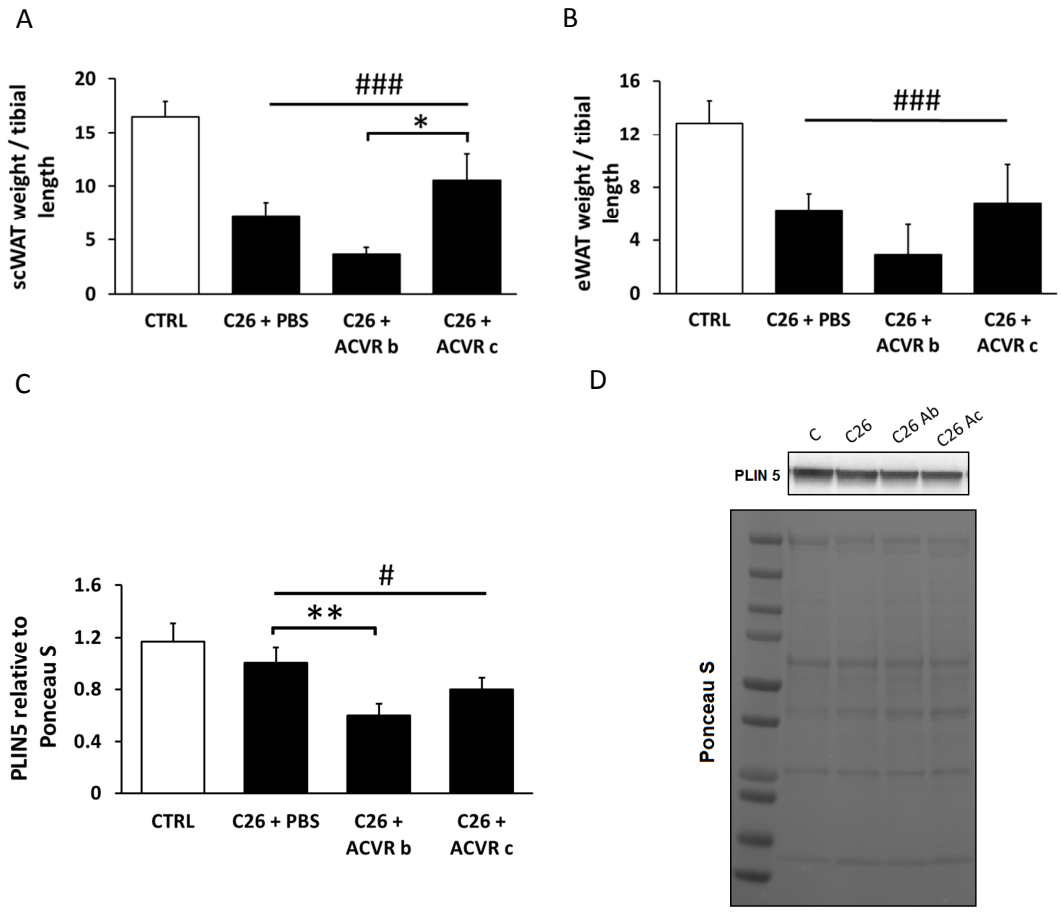

FIGURE 15. A) Subcutaneous white adipose tissue (scWAT) weight normalized to tibial length (mg/mm). * depicts significant difference between the groups designated by lines, $p < 0.05$. ### depicts significant negative cancer effect, $p < 0.001$, $n = 9$ in CTRL group, 7-8 in others. B) Epididymal white adipose tissue (eWAT) weight normalized to tibial length (mg/mm). ### depicts significant negative cancer effect, $p < 0.001$, $n = 9$ in CTRL group, 7-8 in others. C) PLIN5 at protein level. ** depicts significant difference between the groups designated by lines, $p < 0.01$. # depicts negative cancer effect $p < 0.05$, $n = 6$ in C26 + ACVR b, 7-8 in others. D) PLIN5 normalized to Ponceau S.

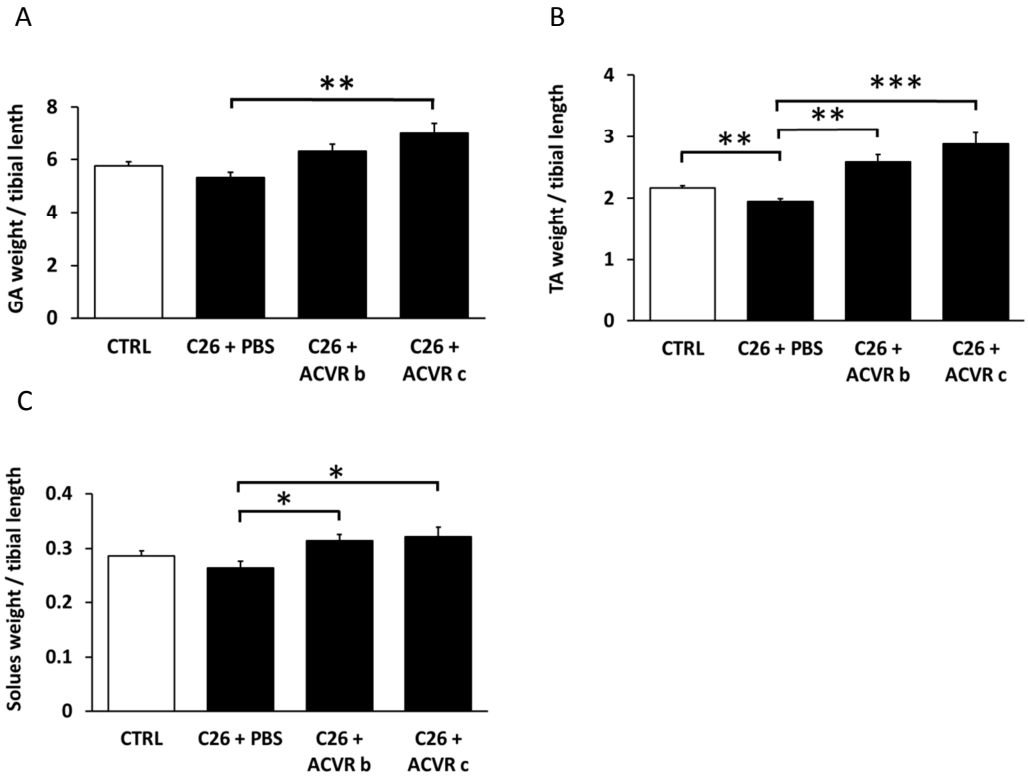

FIGURE 16. A) Gastrocnemius (GA) weight normalized to tibial length (mg/mm). ** depicts significant difference between the groups designated by lines, $p < 0.01$. B) Tibialis anterior (TA) weight normalized to tibial length (mg/mm). ** or *** depicts significant difference between the groups designated by lines ($p < 0.01$ and $p < 0.001$, respectively). C) Soleus weight normalized to tibial length (mg/mm). * depicts significant difference between the groups designated by lines, $p < 0.05$. In all the muscle figures n = 9 in CTRL group, 7-8 in others.

The significant decrease in scWAT mass due to the C26 changes the proportion of RNA, protein and TGs in the adipose tissue (Figure 15A and 17A-B). There is a significant cancer effect in the increase of RNA ($p < 0.001$) and protein ($p < 0.01$) yield as when the adipose tissue mass decreases the proportion of RNA and protein increases in the fat tissue (Figure 17A-B). Pearson correlation between RNA yield and scWAT/TL was -0.522 ($p < 0.003$, $R^2 = 0.472$) and protein yield and scWAT/TL -0.329 ($p < 0.024$, $R^2 = 0.264$). Pearson correlation results are shown in Figure 17C-D.

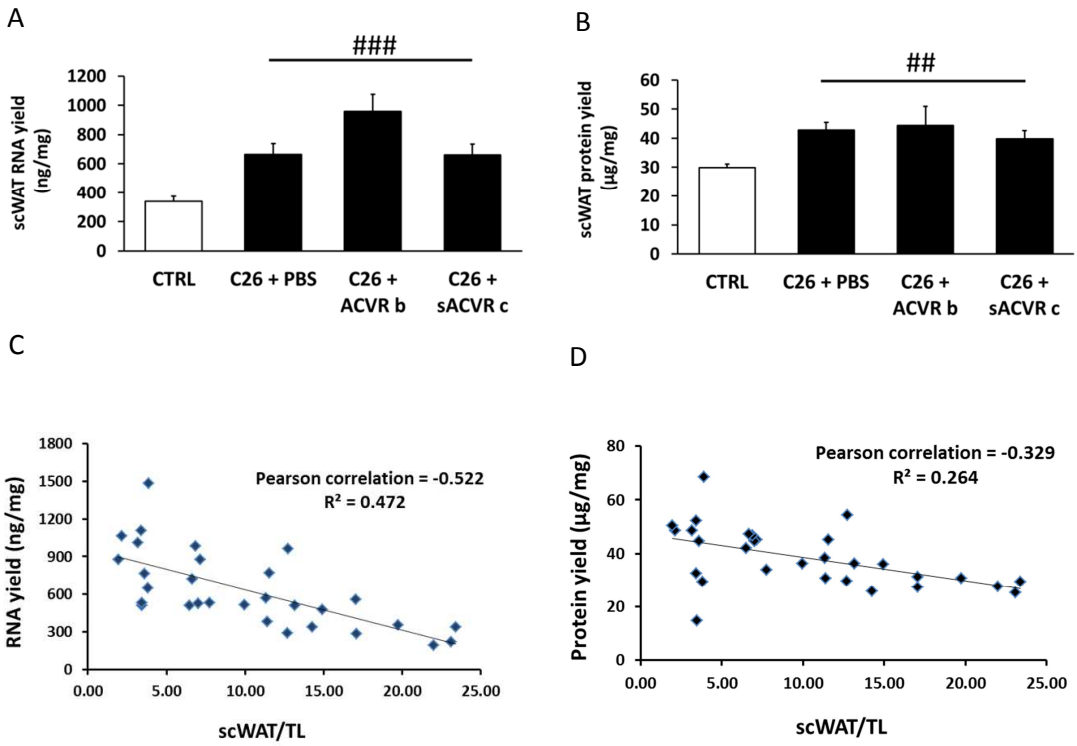

FIGURE 17. A) RNA yield from scWAT. ### depicts significant positive cancer effect, $p < 0.001$. B) Protein yield from scWAT. ## depicts significant positive cancer effect, $p < 0.01$. C) Pearson correlation of RNA yield and scWAT/TL, $p = 0.003$, $R^2 = 0.472$. D) Pearson correlation of protein yield and scWAT/TL, $p = 0.024$, $R^2 = 0.264$. In all figures n = 9 in CTRL group, 7-8 in others.

8.2 White adipose tissue browning markers

The results of WAT browning markers show variation at the mRNA level. Browning outcome marker UCP1 is significantly decreased in all the cancer groups showing a cancer effect ($p < 0.001$) (Figure 18A). At protein level the UCP1 result is similar; there is a clear negative cancer effect compared to the control ($p < 0.01$) (Figure 18C). Continued sACVR2B-Fc treatment increased UCP1 protein expression slightly when compared to PBS group ($p < 0.05$), yet remaining at lower level than the control group (significance not shown in Figure 18C). At mRNA level, PGC-1α1 isoform and PRDM16 were increased in the cancer when compared to control group ($p < 0.001$ and $p < 0.05$, respectively) (Figure 18B and Figure 19A). Increase of PGC-1α1 at mRNA level did not cause any changes at protein level of PGC-1α (Figure 18D). DIO2 showed no significant differences between groups at mRNA level (Figure 19B).

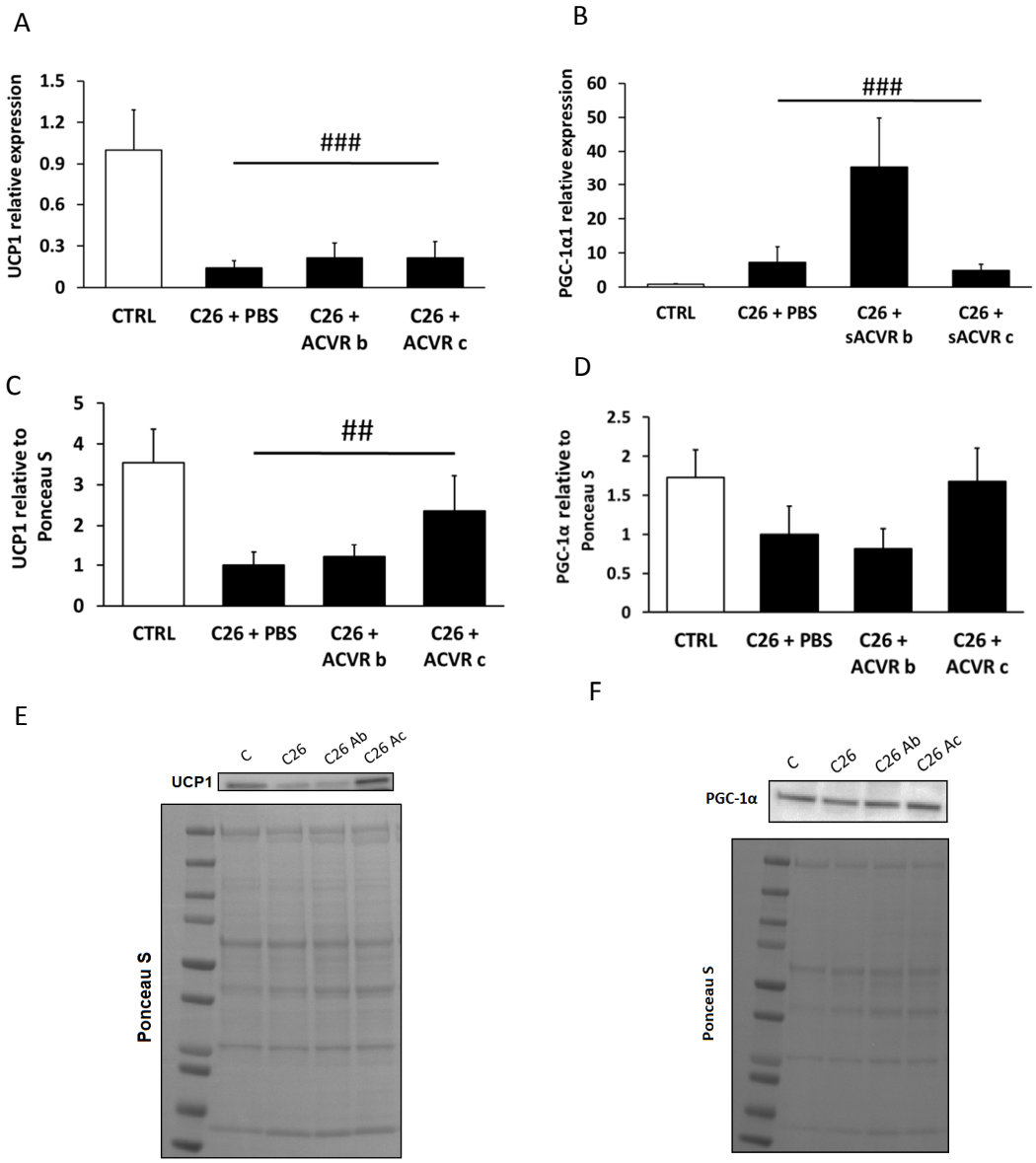

FIGURE 18. WAT browning markers at mRNA and protein level. A) UCP1 at mRNA level. ### depicts significant negative cancer effect, $p < 0.001$. B) PGC-1α1 at mRNA level. ### depicts significant positive cancer effect, $p < 0.001$. C) UCP1 at protein level. ## depicts significant negative cancer effect, $p < 0.01$, $n = 4$ in C26 + PBS, $n = 5$ in C26 + ACVR b and $n = 6$ in CTRL and AVCR c. D) PGC-1α at protein level does not show any differences, $n = 6$ in C26 + PBS and C26 + ACVR c and $n = 7$ in CTRL and C26 + ACVR b. E) UCP1 normalized to Ponceau S. F) PGC-1α normalized to Ponceau S.

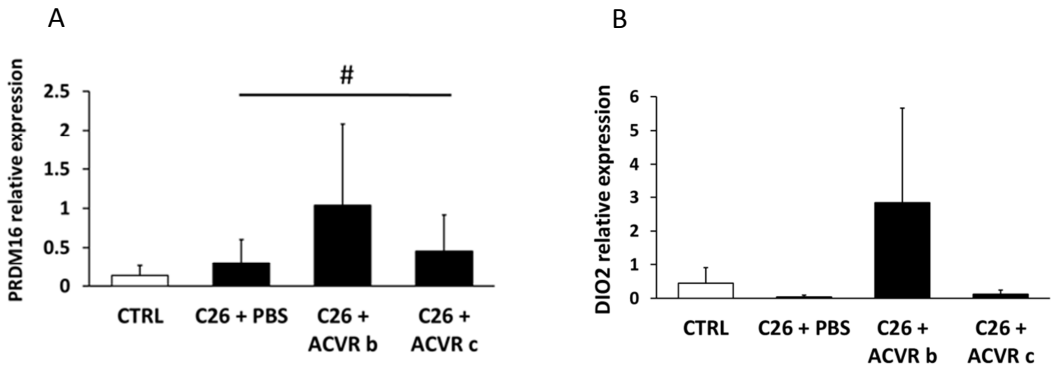

FIGURE 19. A) PRDM16 at mRNA level. # depicts significant positive cancer effect, $p < 0.05$, n = 6 in C26 + PBS and C26 + ACVR b and n= 7 in CTRL and C26 + ACVR c. B) DIO2 shows no differences at mRNA level, n = 6 in CTRL, n = 7 in C26 + PBS and C26 + ACVR b and n = 8 in C26 + ACVR c.

8.3 Mitochondrial function

Citrate synthase activity remained stable in cancer and the sACVR2B-Fc treatment did not have any effect on it (Figure 21). Oxidative phosphorylation remained functional but there was a decreasing trend ($p < 0.052$) in total OXPHOS suggesting a slight negative cancer effect at this time point (Figure 22A). sACVR2B-Fc treatment had no additional effect on total OXPHOS. Complex V of the OXPHOS showed a mild negative cancer effect ($p < 0.05$, data not shown). Cytochrome *c* was in line with other mitochondrial results showing no significant changes between study groups (Figure 22C). In skeletal muscle (TA) there were not significant differences between groups in total OXPHOS, Cytochrome *c*, ACC or PDK4 (data not shown).

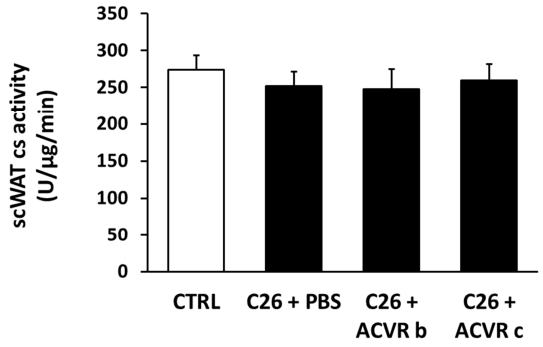

FIGURE 21. Citrate synthase activity of scWAT the experiment showed no differences between groups at the end of the study. In CTRL group n = 9, 7-8 in others.

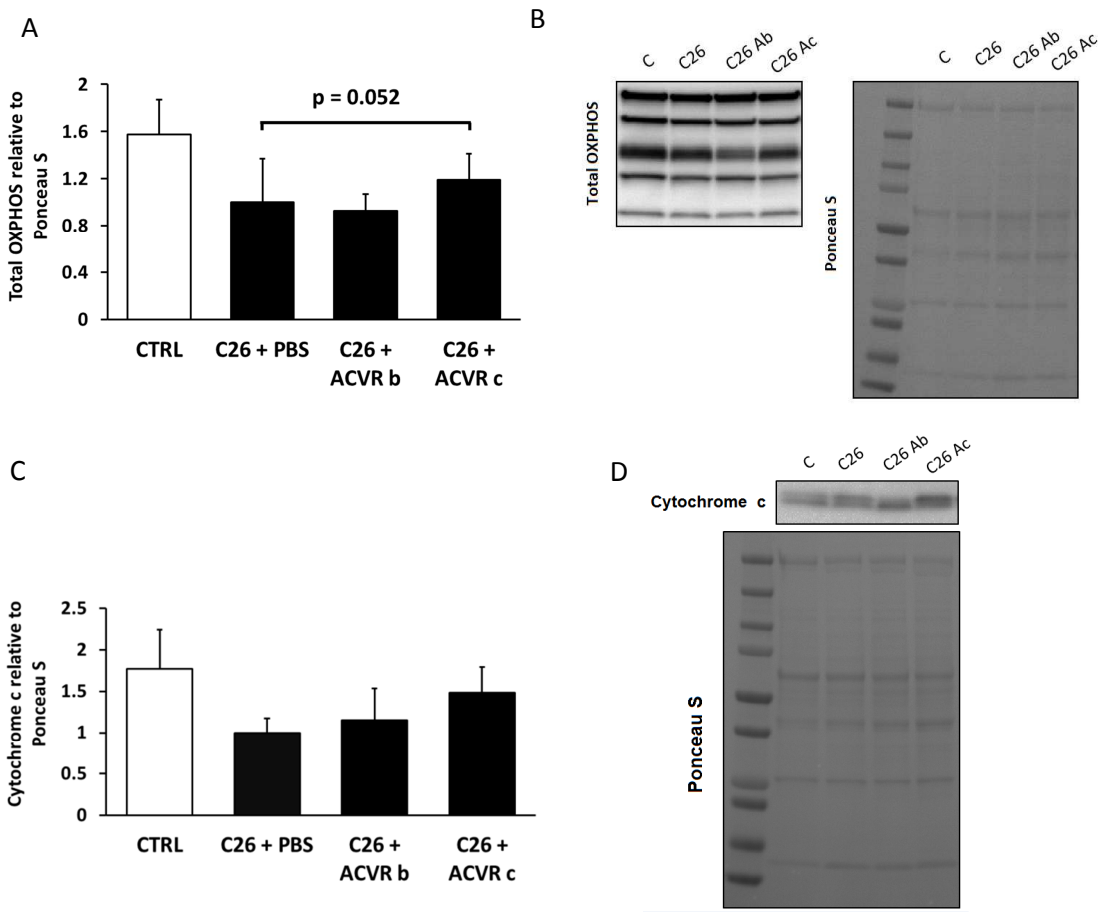

FIGURE 22. A) Total OXHOS at protein level. There is a negative cancer effect trend in total OXPHOS, p = 0.052. B) Total OXPHOS normalized Ponceau S. C) Cytochrome *c* shows no differences at protein level, n = 6 in C26 + ACVR b, 7-8 in others. D) Cytochrome *c* normalized to Ponceau S.

8.4 Lipolysis and lipogenesis

Phosphorylation of the lipases (ATGL and HSL) was not changed nor had the sACVR2B-Fc treatment any effect on it. sACVR2B-Fc treatment before C26 cell injection showed a slight but not significant decrease in ATGL protein level when compared to cancer alone (C26 + PBS) but the continued treatment did not have the same effect (Figure 23A). Similarly to ATGL, HSL phosphorylation remained at control level in all the groups without showing any significant changes (Figure 24A). Only p-HSL (Ser660) was slightly decreased in continued sACVR2B-Fc treatment group compared to cancer alone (C26 + PBS), $p < 0.05$. The phosphorylation of the acetyl CoA carboxylase (ACC) of all the cancer groups remained at the same level as the control group without showing any significant differences (Figure 25A).

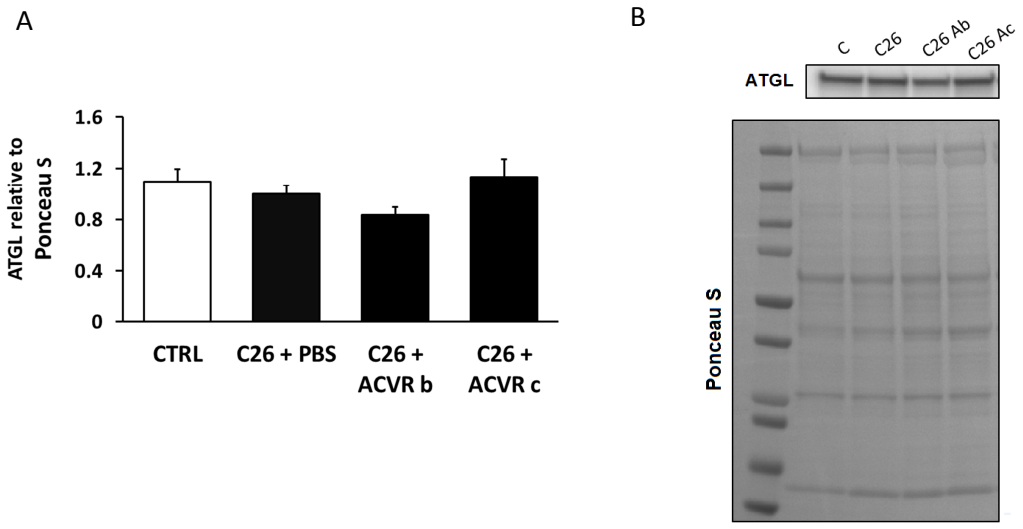

FIGURE 23. A) ATGL at protein level shows no significant differences between groups. B) ATGL normalized to Ponceau S.

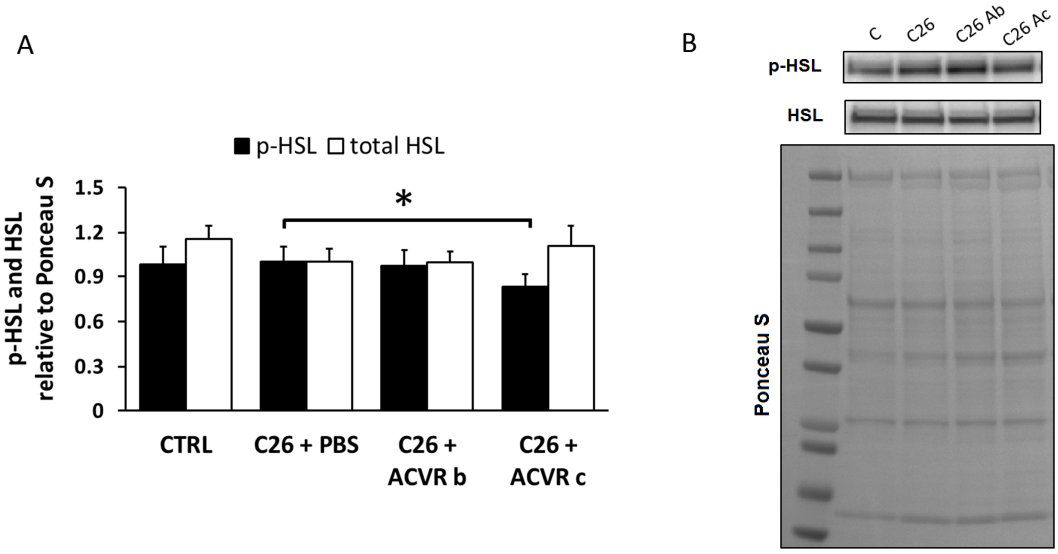

Figure 24. A) p-HSL (Ser660) and HSL. * depicts significant difference between the groups designated by lines, $p < 0.05$. In p-HSL n = 6 in C26 + ACVR b, 7-8 in others. B) p-HSL and HSL normalized to Ponceau S.

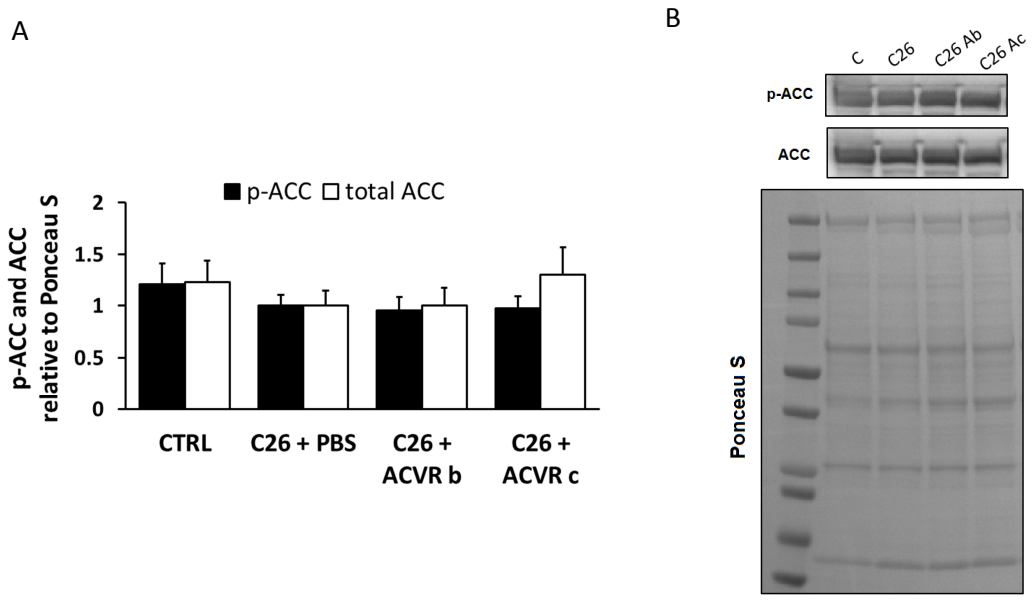

FIGURE 25. A) p-ACC and ACC show no statistical differences at protein level. In p-ACC n = 6 in C26 + ACVR b, 7-8 in others. B) p-ACC and ACC normalized to Ponceau S.

8.5 Inflammation and IL-6

In agreement with previous studies with the same murine model, there was a significant positive cancer effect of IL-6 and p-STAT3 signaling in C26 cancer. At protein level phosphorylation of STAT3 had a clear positive cancer effect between groups ($p < 0.001$) (Figure 26A). Changes in total STAT3 was not observed which explains a significant increase of p-STAT3 per STAT3 in cancer groups vs. control group ($p < 0.001$) (Figure 26C). Upstream to STAT3, IL-6 expression at mRNA level was significantly higher due to the cancer effect ($p < 0.01$) (Figure 26D). A significant increase in IL-6 expression in the tumor itself and skeletal muscle was found thus suggesting that in C26 IL-6 is not only a tumorkine but also a myokine and an adipokine as is previously already been shown (data not shown). sACVR2B-Fc treatment seems to increase IL-6 expression at mRNA level but has no effect on protein levels of STAT3, but p-STAT3 increases above the cancer effect in before treated sACVR2B group than in continued treatment group.

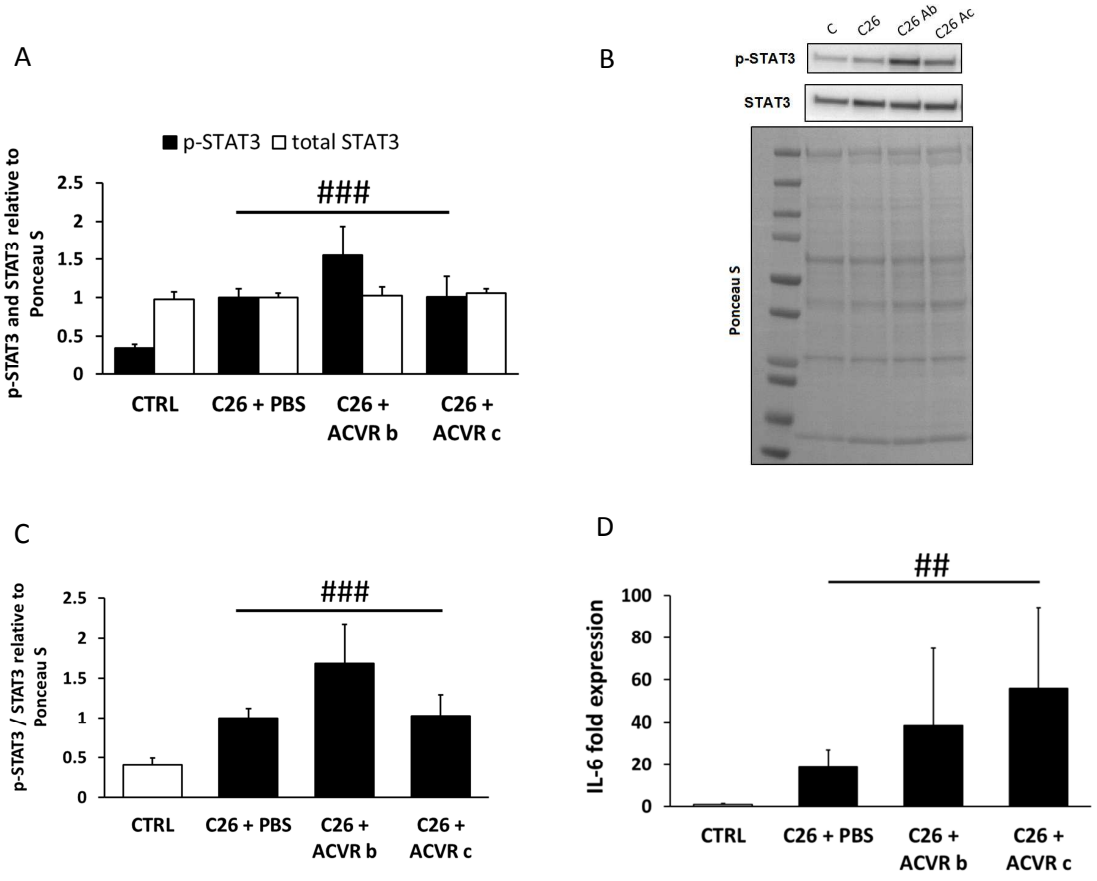

FIGURE 26. A) p-STAT3 and total STAT3. ### depicts significant positive cancer effect of p-STAT3, $p < 0.001$. B) p-STAT3 and STAT3 normalized to Ponceau S. C) p-STAT3 per STAT3. ### depicts significant positive cancer effect, $p < 0.001$. D) IL-6 mRNA expression, $n = 7$ in CTRL group, $n = 7$ in others. ## depicts significant positive cancer effect, $p < 0.01$.

8.6 Intramyocellular triacylglycerol content

To investigate the effects of C26 and blockade of the ACVR2B pathway on intramyocellular lipid content, gastrocnemius muscle TGs were measured. C26 caused a significant decrease in the GA triacylglycerol content when all the cancer groups together were compared to the control group ($p < 0.01$) (Figure 27). sACVR2B-Fc treatment did not have any effect on triacylglycerol accumulation into the skeletal muscle beyond the cancer effect, at least at this time point, although results suggest that continuous sACVR2B-Fc treatment preserved TGs better than if treatment was ended at the time of the C26 cell inoculation ($p < 0.05$).

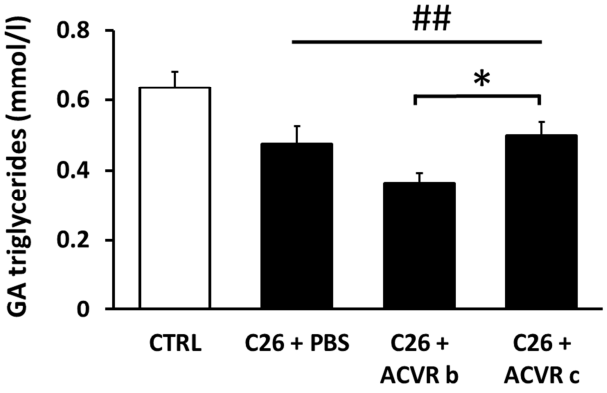

FIGURE 27. Triacylglycerol content in the gastrocnemius muscle. * depicts significant difference between the groups designated by lines, $p < 0.05$. ## depicts significant negative cancer effect, $p < 0.01$. In CTRL group n = 9, 7-8 in others.

9 DISCUSSION

The primary aim of the study was to determine if WAT browning occurs in early cachexia and if the sACVR2B-Fc treatment has any effect on this phenomenon. Secondary aim was to determine whether TGs accumulate into skeletal muscle in early cachexia and does sACVR2B-Fc treatment affect this. Three C26 tumor-bearing mice groups (C26 + PBS, C26 + ACVR before cancer cell inoculation and C26 + AVCR continued after cancer cell inoculation) and a healthy control group (n = 9 per group) were observed for 13 days before and 11 days after C26 cell inoculation resulting overall duration of the experiment to be 24 days. The main result of this experiment was that neither WAT browning nor TG accumulation were observed in early C26 preclinical cachexia and that sACVR2B-Fc treatment does not have any additional effects on either phenomenon. These results support the theory that WAT browning may not yet occur or may not be as important in adipose tissue atrophy and weight loss in early cachexia as previously has been assumed. Significant adipose tissue atrophy was observed at day 11 in C26 bearing mice with decreased physical activity levels accompanied with no consistent effects on mitochondrial count.

Body composition, activity and food consumption. C26 alone caused significant changes in body composition by causing skeletal muscle wasting and especially adipose tissue atrophy as it has previously been shown with this same model (De Larichaudy et al. 2012; Murphy et al. 2012). Muscle atrophy caused by C26 was prevented by sACVR2B-Fc treatment and this increased the body weight of the cachectic mice as was expected and shown previously (Zhou et al. 2010). WAT was wasted at same rate with or without the receptor blocker treatment which suggests that sACVR2B-Fc treatment does not have any additional enhancing effect on lipolysis and lipid metabolism in adipose tissue or in skeletal muscle in early cachexia.

Physical activity and food consumption followed a similar pattern as when food consumption started to decrease so did the activity, a finding already observed previously by others (Toledo et al. 2015). As well, physical activity decreases in cancer in animals and in humans (Toledo et al 2011; Moses et al. 2004). Many of the cachectic patients may have to stay in bed rest due to illness which decreases physical activity, muscle function and suppresses protein synthesis. This may also explain muscle atrophy in cachexia as the rate of protein degradation exceeds the protein synthesis due to e.g. increased catabolic mechanism and lack of anabolic stimuli

(Gullet et al. 2011; Gould et al. 2013). As well, other factors such as decreased plasma insulin level and/or insulin sensitivity of the skeletal muscle, lowered protein translation rate or inadequate pool of different amino acids due to lowered appetite may downregulate muscle protein synthesis. Physical activity decreases inflammation, improves muscle strength and function and increases quality on life and as the cachectic mice become less active towards the end of the study, it suggests that benefits of the exercise are lost in cachexia if activity is not voluntarily maintained. (Gould et al. 2013). Although the number of clinical trials is small, a few human studies have shown that cachectic patients benefit from resistance training which prevents muscle atrophy and loss of the muscle function which occurs in non-exercising cachectic patients (Segal et al. 2003; Segal et al. 2009). It seems that there is a pattern starting from decreased physical activity due to lack of adequate nutrient intake and muscle fatigue in early cachexia developing towards muscle and adipose tissue wasting thus lowering the survival expectancy (Gullet et al. 2011). This supports the results of physical activity as decreased activity and food consumption probably in part caused muscle atrophy in placebo cancer group but sACVR2B-Fc treatment prevented this by preserving the muscle mass without preventing adipose tissue wasting. Yet, decrease in eating alone cannot explain the significant adipose tissue wasting of the cancer groups as also physical activity decreased to similar extent.

Cachexia cannot be overcome by basic nutritional interventions and cancer patients have often reduced food consumption due to e.g. altered hormonal regulation and poor physical condition. Nutrient and vitamin intake may decrease due to nausea and vomiting resulting in negative energy balance and tissue loss. (Das et al. 2011; Gould et al. 2013; Penet & Bhujwalla 2015). Human studies have shown that nutritional support may have even unwanted outcomes as hyperglycemia is commonly observed, at least in early studies with parenteral nutrition. The problem with nutritional studies in cancer patients is the lack of carefully randomized controlled clinical trials. (Gullet et al. 2011). Decrease in energy intake partially explains weight loss in cachexia but some other underlying mechanisms interfere with energy homeostasis as well because e.g. increased pro-inflammatory cytokine release cannot be explained by anorexia (Müller et al. 2010). This suggests that futile cycles e.g. Cori cycle and other energy demanding processes require too much energy that normal eating would be enough to satisfy that need.

As adipose tissue mass was decreased, RNA and protein yield increased significantly. This is logical as when the TG content of the adipocyte decreases, the proportion of RNA, protein

and DNA increases. Most clearly this was seen in control group as the greater the fat mass was, the lower the RNA and protein yield was and *vice versa*. Variation in this could be explained at some rate by human studies (Batista et al. 2015; Alves et al. 2017) showing infiltration of the inflammatory cells into the WAT accompanied with increased fibrosis of adipose tissue during cachexia of gastrointestinal patients. This could contribute to increased RNA and protein yield in cachexia. Interestingly, greatest level of phosphorylated STAT3 was in the same group that showed greatest RNA and protein yield increase. IL-6 expression at mRNA level was not greatest in this same group, but elevated still significantly.

WAT browning markers. Unlike some previous studies with LLC, C26 and B16 cancers (Kir et al 2014; Petruzzelli et al. 2014), WAT browning was not observed in this study. UCP1 was downregulated at protein and mRNA level suggesting that lack of adequate signal for WAT browning at this time point is missing, but cachexia and adipose tissue wasting have still occurred. 11 days may be too brief time for UCP1 to have been increased at mRNA and protein level in adipose tissue so that it would influence WAT browning and atrophy. As well, if this was the case, now it should have been downregulated and signs of mitohcondriogenesis should be detectable, which was not the case not observed. At mRNA level PRDM16 had slight cancer effect and DIO2 was unaltered so there is no consistent enhancement of WAT browning marker gene expression. sACVR2B-Fc treatment did not have any effect on the expression of the WAT browning markers although it has previously been shown to enhance WAT browning (Zhang et al. 2012; Shan et al. 2013; Singh et al. 2014). Loss of function of TGF-β-activated kinase 1 (TAK1) also increases WAT browning thus emphasizing the role of TGF-β family members and ACVR2B pathway in WAT gene expression (Sassmann-Schweda et al. 2016). Fat browning regulator PGC-1α was unchanged at protein level accompanied with slight increase at mRNA level. Supporting the present results, browning of WAT was not detected by Kliewer et al. (2015) at early cachexia in C26 mice. This might be due to different duration of other studies or different ending criteria. The results suggest that WAT browning may not be as common or important phenomenon in cancer related adipose tissue wasting supporting the theory recently suggested by Rohm et al. (2016). Instead, loss of the adipose tissue and increased energy expenditure could occur through simultaneous induction of both lipolytic and lipogenic pathways (Rohm et al. 2016). However, at day 11 it was perhaps too late to observe the changes in these pathways.

Mitochondrial function. Protein level of Cytochrome *c* and activity of citrate synthase were unaltered in subcutaneous fat between study groups. Total OXPHOS was mildly affected by

the cancer suggesting possibly slightly decreased mitochondrial oxidative capacity in early cancer. Overall, mitochondrial count at this time point remained normal and sACVR2B-Fc did not affect the WAT browning or mitochondriogenesis. UCP1 production was not increased so most likely thermogenesis and browning have not occurred in scWAT at this time point. PGC-1α was elevated at mRNA level but not at protein level so maybe there was a signal to enhance mitochondriogenesis but it was not observed at this time point at functional level of mitochondria.

Lipolysis and lipogenesis. Unlike in other studies (Das et al. 2011; Henriques et al. 2017), neither lipolysis nor lipogenesis were altered in this study, although significant amount of adipose tissue was lost already at day 11 referring to early cachexia. ATGL and total HSL remained unaltered in all the study groups and p-HSL (ser660) showed even a negative cancer effect. As the amount of adipose depots was strongly decreased in all cancer groups, there is a possibility that lipolysis was promoted at earlier time point and now this pathway is silenced as no more TGs are left in adipose tissue. Lipogenesis and acetyl CoA carboxylase were unaltered in cancer groups compared to control as is suggested by previous studies as lipolysis is considered to be main contributor of adipose tissue loss, not the impaired lipogenesis. (Tsoli & Robertson 2013; Petruzzelli & Wagner 2016). In some other studies, however, impaired lipogenesis was suggested to also affect adipose tissue loss due to WAT browning markers (Tsoli et al. 2016; Henriques et al. 2017).

Inflammation and IL-6 signaling. Consistent with previous studies using the C26 (Bonetto et al. 2011; Tsoli et al. 2016), elevated IL-6 signaling at mRNA and protein level via downstream STAT3 signaling was observed. Similarly, IL-6 mRNA expression in the tumor was increased as well (data not shown). Human study of gastrointestinal patients has shown that IL-6 expression in WAT did not increase during cachexia although plasma IL-6 concentration was elevated thus suggesting that IL-6 may not act as an adipokine in humans (Rydén et al. 2008).

Increased IL-6 activity in cachexia has been related to muscle wasting and liver acute phase response although it is not the only cytokine related to the phenomenon (Tsoli et al. 2016; Bonetto et al. 2011; Fearon et al. 2012). Normally IL-6 regulates energy homeostasis and substrate utilization and if this signaling now is impaired, it raises a question if IL-6 could cause imbalances to the energy metabolism during cachexia. Overexpression of IL-6 has been shown to increase sympathetic activity in hypothalamus and thus enhance UCP1 expression

and thermogenic ability of BAT increasing energy expenditure. (Tsoli et al 2016). In this study energy expenditure was not measured, but cancer groups showed significantly decreased physical activity and increased adipose tissue wasting but food intake decreased only at the end of the study. This suggests that in cancer group either thermogenesis in BAT or other futile cycles are enhanced, releasing energy for e.g. synthesis of liver acute phase response proteins or some other pathways. On the other hand, increased energy expenditure and altered metabolic rate may not explain body and adipose tissue loss as cancer patients can be hypo-, normo- or hyper-metabolic. Nor does the size or the energy and fuel demand of the tumor explain the weight loss as very small tumors can cause cachexia as larger may not. (Bonetto et al. 2011). In this study tumor size was small and did not differ between the PBS and sACVR2B-Fc groups.

Muscle triacylglycerol content. During cancer, lipid accumulation into skeletal muscle has previously been shown in LLC murine model (Das et al. 2011) and upper gastrointestinal (oesophageal, gastric and pancreatic) cancers in humans (Stephens et al. 2011). In early cachexia lipid accumulation was not observed in C26 cancer bearing mice (Kliewer et al. 2015). Same way as Kliewer et al. (2015), triacylglycerol accumulation into skeletal muscle in early cachexia was not observed in this study. Decrease in intramyocellular TGs is in line with the overall adipose tissue mass loss in early cachexia suggesting enhanced lipid turnover and mobilization of all the adipose depots of the body. The decrease in triacylglycerol content in GA supports these findings and may suggest that all the infiltrated muscle FAs are used to energy demanding processes and no buildup is detected.

Limitations and strengths of the study. One limiting aspect of this study is the circadian nature of many of the WAT browning markers, e.g. UCP1 and PRDM16 (Tsoli et al. 2016). In tissue collection and other time points this was tried to be overcome so that in the morning and afternoon euthanization there was a member of all the study groups present. Due to great deviations of RT-qPCR results all the differences between groups were not significant. All the results were analyzed in SPSS with Mann-Whitney U-test and the results were corrected with Holm-Bonferroni method to decrease statistical type 1 error.

Inclusion of one extra group to the study design would have increased the knowledge of effects of sACVR2B-Fc only on WAT browning, adipose tissue atrophy and skeletal muscle lipid handling as now we had two cancer groups that were injected with sACVR2B-Fc either before or both before and after the C26 cell inoculation. The amount of subcutaneous WAT in

some of the cachectic mice was very small and to be confident that the removed sample is adipose tissue, histological staining could have resolved the problem. This was not done due to small sample size and prioritization of RT-qPCR and Western blots. Similar problem was with skeletal muscle triacylglycerol content measurements. Histological measurements could have shown that the sample contained lipid droplets so that the results are from intramyocellular triacylglycerol depots. In the worst case, there could be some adipose tissue on the skeletal muscle surface but in this case, it is not very likely due to small over all adipose tissue mass. As well, inclusion of lipid handling markers from skeletal muscle would have increased the power of the triacylglycerol results.

In Western blots, it would have increased reliability of the results if BAT sample had been used as a positive control for UCP1 and PGC-1α. UCP1 was tested with scWAT pool sample and BAT sample and expected fragments with right size were observed thus increasing the reliability. Control of protein loading in Western blot was Ponceau S but α-Tubulin was also tested but it was not used as it did not work in every run. This may due to same production animal of the primary antibody as e.g. OXPHOS antibody, did not strip and as anti-mouse secondary antibody was used for both, OXPHOS and α-Tubulin, and the sizes of the OXPHOS complex V and α-Tubulin are the same (50 kDa), the latter did not show at all. Also, α-Tubulin was stripped so it produced two fragments instead of one. To avoid this problem one run should have been done so that it was not stripped. This was not done due to limited amount of samples, as the protein concentration of the scWAT was low. Ponceau S normalization has been previously used for adipose tissue in Western blots in other publications, e.g. Higami et al. (2006) and Ramos et al. (2016).

Western blot is a semi-quantitative method due to relative comparison of the protein levels, not the absolute amount of their quantity as protein loading and transfer varies and produced signal in detection is not linear (Mahmood & Yang 2012). Western blot is used to measure expression as well as protein phosphorylation by the help of specifically designed antibodies (Dittmer & Dittmer 2006). Based on this and small number of mice per group the obtained Western blot results must be considered as a strong suggestion what happens in the early cachexia in scWAT. To obtain more support to now observed results of lipid metabolism in early cachexia, the experiment should be replicated and redone by us or others with the same cancer model.

Future prospects of the cancer cachexia treatment. As the cancer cachexia is a multi-organ disease, the treatment and prevention must be multifactorial. Treatments targeting only one aspect or mediator of cachexia have failed to produce the wanted outcome as could be expected in a complex problem. If multiple mediators are causing the disease and their sum is greater than their effect alone, how blocking of only one mediator could prevent the abnormal function of multiple tissues and signaling pathways? Studies of early events of the cancer cachexia could help us to understand the crosstalk and pathophysiology behind the disease and shed light into host-tumor interactions at early stage. (Petruzzelli & Wanger 2016).

Shrinkage of the tumor may attenuate the symptoms of the cancer cachexia but at the moment there is no therapy that could be used to treat humans. (Kir et al. 2014). European Palliative Care Research Collaboration (EPCRC) has developed standard recommendations for treatment of patients with advanced cachexia and these take into account the cachectic state and prognosis of the patient before the start of the treatment as the response time can be weeks rather than days. As the removal of the tumor is not possible in many cases, the main goal of the treatment should then be to prevent weight loss and try to reverse loss of the skeletal muscle mass. The treatment protocol is very similar to pre-cachectic patients and refractory state patients. (Suzuki et al. 2013). In the Table 2 a few potential pharmacological drugs are shown that could have potential to become medical protocol in the treatment of cancer cachexia.

Table 2. Potential treatment strategies in the fight against cancer cachexia. Anamorelin has shown promising results in clinical studies at phase III. All the listed drugs are in clinical studies at phases differing from I to III. (Petruzzelli & Wagner 2016).

Agent	Mechanism of action	Physiological effects
Anamorelin	Ghrelin receptor agonist	Appetite-enhancing and anabolic activity
Bimagrumab	Anti-ActRII monoclonal antibody	Prevent skeletal muscle atrophy
Clazakizumab	Anti-IL-6 monoclonal antibody	Anti-inflammatory activity
Enobosarm	Selective androgen receptor modulator	Anabolic activity
IP-1510	IL-1 receptor antagonist	Anti-inflammatory activity
MABp1	Anti-IL-1α monoclonal antibody	Anti-inflammatory and anti-neoplastic activity
REGN1033	Myostatin antagonizing antibody	Prevents skeletal muscle atrophy

Combination of nutrition and exercise as a treatment approach is recommended for cachectic patients. Medication increasing food intake and appetite (e.g. ghrelin agonist) could maintain tissue mass/function ratio. (Fearon et al. 2012). Anti-ACVR2B blockade that inhibits activins has been tested and shown to be effective against cancer cachexia in mice even when

combined with anti-cancer therapies which is also promising result from the human perspective (Penet & Bhujwalla 2015; Hatakeyama et al. 2016). By blocking members of the TGF-β family could prevent further muscle atrophy and even reverse skeletal muscle wasting. This increases the rate of survival and promotes better quality of life for the cancer patients. As adipose tissue wasting was not inhibited nor it affected the results of anti-ACVR2B therapy in mice, it seems that preventing skeletal muscle loss may be more important than preventing adipose tissue loss. Combination of muscle wasting prevention and nutritional support e.g. appetite increasing factors like ghrelin could possibly increase the survival rate. Now in this study the skeletal muscle mass was increased and maintained by chemical support but in the future it would be interesting to see how muscles build by lifetime of physical activity and exercise would response to cancer accompanied with sACVR2B-Fc treatment. Disadvantage of the exercise on adipose tissue is that it does not prevent and can even enhance WAT wasting which could be detrimental on energy homeostasis and normal hormonal function. Still, the complexity behind the pathophysiology of cancer cachexia makes it difficult to point out one major regulator that is causing the disease. Most likely there are many regulators interfering with each other to mediate their outcome. (Tisdale 2010; Zhou et al. 2010). In the future human research one should take into consideration at least three different perspectives of cachexia; the type/location of the tumor and tumor derived cytokines, response of the host (e.g. inflammation and immune changes) to tumor burden and additional effect of the other given anti-cancer treatments (e.g. chemotherapy and/or surgery). Overall more research effort should be directed in the future to study WAT browning in humans and determine if that occurs or if this phenomenon has any contribution to human cancer cachexia. Now the topic is mostly studied by murine cancer models and always those results are not directly usable to human diseases. This emphasizes the importance of the research in this area as well as the difficulty of finding the effective treatment for the cancer cachexia.

10 CONCLUSIONS

Cancer cachexia is related to adipose tissue and skeletal muscle loss accompanied with reduced physical activity and feed intake both in animal and human (Zhou et al 2010; Segal et al. 2003; Gould et al. 2013; Petruzzelli et al. 2014). White adipose tissue browning has previously been thought to partially cause the adipose tissue atrophy but in this study this phenomenon was not observed in early cachexia in Colon-26 murine model. The blockade of the ACVR2B pathway did not cause strong enough stimulus to enhance white adipose tissue browning nor did it further promote adipose tissue atrophy in early cachexia even when the sACVR2B-Fc treatment was continued. The results support the theory suggested by Rohm et al. (2016) that WAT browning as an enhancer of adipose tissue wasting may not be as common symptom in cachexia as has previously been expected.

Activity of all the cachectic mice was reduced towards the end of the study regardless of the muscle or adipose tissue mass gain or atrophy, respectively. This suggests that although muscles remain larger, other factors may decrease the physical activity. sACVR2B-Fc treatment did not have any effect on level of physical activity although it reserved skeletal muscle mass.

Similarly to adipose tissue wasting, triacylglycerol accumulation into skeletal muscle did not occur in early cachexia. The blockade of the ACVR2B pathway did not have any additional effect on lipid metabolism in the skeletal muscle.

REFERENCES

Acharyya, S., Ladner, K.J., Nelsen, L.L., Damrauer, J., Reiser, P.J., Swoap, S., & Gurrridge D.C. 2004. Cancer cachexia is regulated by selective targeting of skeletal muscle gene products. The Journal of clinical investigation, 114(3), 370-378.

Anandavadivelan, P & Lagergren, P. 2016. Cachexia in patients with oesophageal cancer. Nature Reviews Clinical Oncology, 13(3), 185-198.

Argilés, J. M., Busquets, S., Stemmler, B., & López-Soriano, F. J. 2014. Cancer cachexia: understanding the molecular basis. Nature reviews Cancer,14(11), 754-762.

Argilés J. M., Stemmler, B., López-Soriano, F. J., & Busquets, S. 2015. Nonmuscle Tissues Contribution to Cancer Cachexia. Mediators of Inflammation, 2015, 182872.

Badin, P. M., Louche, K., Mairal, A., Liebisch, G., Schmitz, G., Rustan, A. C., ... & Moro, C. 2011. Altered skeletal muscle lipase expression and activity contribute to insulin resistance in humans. diabetes, 60(6), 1734-1742.

Betz, M. J., & Enerbäck, S. 2015. Human brown adipose tissue: what we have learned so far. Diabetes, 64(7), 2352-2360.

Bing, C., & Trayhurn, P. 2009. New insights into adipose tissue atrophy in cancer cachexia. Proceedings of the Nutrition Society, 68(04), 385-392.

Bonetto, A., Aydogdu, T., Kunzevitzky, N., Guttridge, D. C., Khuri, S., Koniaris, L. G., & Zimmers, T. A. 2011. STAT3 activation in skeletal muscle links muscle wasting and the acute phase response in cancer cachexia. PloS one, 6(7), e22538.

Bossola, M., Marzetti, E., Rosa, F., & Pacelli, F. 2016. Skeletal muscle regeneration in cancer cachexia. Clinical and Experimental Pharmacology and Physiology, 43(5), 522-527.

Bournat, J. C., & Brown, C. W. 2010. Mitochondrial dysfunction in obesity. Current opinion in endocrinology, diabetes, and obesity, 17(5), 446.

Brown adipose tissue. Klingenspor, M. & Fromme, T. In a book: Symonds, M. E. (ed.). 2012. Adipose tissue biology. Springerlink, New York, USA. pp 44 (https://jyu.finna.fi/Record/jykdok.1249273)

Bruce, C. R., Brolin, C., Turner, N., Cleasby, M. E., van der Leij, F. R., Cooney, G. J., & Kraegen, E. W. 2007. Overexpression of carnitine palmitoyltransferase I in skeletal muscle in vivo increases fatty acid oxidation and reduces triacylglycerol

esterification. American Journal of Physiology-Endocrinology and Metabolism, 292(4), E1231-E1237.

Cao, L., Choi, E. Y., Liu, X., Martin, A., Wang, C., Xu, X., & During, M. J. 2011. White to brown fat phenotypic switch induced by genetic and environmental activation of a hypothalamic-adipocyte axis. Cell metabolism,14(3), 324-338.

Chen, J. L., Walton, K. L., Winbanks, C. E., Murphy, K. T., Thomson, R. E., Makanji, Y., ... & Gregorevic, P. 2014. Elevated expression of activins promotes muscle wasting and cachexia. The FASEB Journal, 28(4), 1711-1723.

Chondronikola, M., Volpi, E., Børsheim, E., Porter, C., Annamalai, P., Enerbäck, S., ... & Yfanti, C. 2014. Brown adipose tissue improves whole-body glucose homeostasis and insulin sensitivity in humans. Diabetes, 63(12), 4089-4099.

Cohen, P., & Spiegelman, B. M. 2016. Cell biology of fat storage. Molecular Biology of the Cell, 27(16), 2523-2527.

Dalen, K. T., Dahl, T., Holter, E., Arntsen, B., Londos, C., Sztalryd, C., & Nebb, H. I. 2007. LSDP5 is a PAT protein specifically expressed in fatty acid oxidizing tissues. Biochimica et Biophysica Acta (BBA)-Molecular and Cell Biology of Lipids, 1771(2), 210-227.

Das, S. K., Eder, S., Schauer, S., Diwoky, C., Temmel, H., Guertl, B., .. & Zimmermann, R. 2011. Adipose triglyceride lipase contributes to cancer-associated cachexia. Science, 333(6039), 233-238.

Das, S. K., & Hoefler, G. 2013. The role of triglyceride lipases in cancer associated cachexia. Trends in Molecular Medicine, 19(5), 292–301.

De Larichaudy, J., Zufferli, A., Serra, F., Isidori, A. M., Naro, F., Dessalle, K., ... & Lefai, E. 2012. TNF-α-and tumor-induced skeletal muscle atrophy involves sphingolipid metabolism. Skeletal muscle, 2(1), 2.

Dittmer, A., & Dittmer, J. 2006. β□Actin is not a reliable loading control in Western blot analysis. Electrophoresis, 27(14), 2844-2845.

Doolittle, M. H., Wong, H., Davis, R. C., & Schotz, M. C. 1987. Synthesis of hepatic lipase in liver and extrahepatic tissues. Journal of lipid research, 28(11), 1326-1334.

Ebadi, M., & Mazurak, V. C. 2014. Evidence and Mechanisms of Fat Depletion in Cancer. Nutrients, 6(11), 5280–5297.

Eibl, G. 2008. The Role of PPAR-γ and Its Interaction with COX-2 in Pancreatic Cancer. PPAR Research, 2008, 326915.

Evans, W. J., Morley, J. E., Argilés, J., Bales, C., Baracos, V., Guttridge, D., ... & Marks, D. 2008. Cachexia: a new definition. Clinical nutrition, 27(6), 793-799.

Fearon, K. C., Glass, D. J., & Guttridge, D. C. 2012. Cancer cachexia: mediators, signaling, and metabolic pathways. Cell metabolism, 16(2), 153-166.

Fouladiun, M., Körner, U., Bosaeus, I., Daneryd, P., Hyltander, A., & Lundholm, K. G. 2005. Body composition and time course changes in regional distribution of fat and lean tissue in unselected cancer patients on palliative care—correlations with food intake, metabolism, exercise capacity, and hormones. Cancer, 103(10), 2189-12

Fournier, B., Murray, B., Gutzwiller, S., Marcaletti, S., Marcellin, D., Bergling, S., ... & Hatakeyama, S. 2012. Blockade of the activin receptor IIb activates functional brown adipogenesis and thermogenesis by inducing mitochondrial oxidative metabolism. Molecular and cellular biology, *32*(14), 2871-2879.

García-Alonso, V., & Clària, J. 2014. Prostaglandin E_2 signals white-to-brown adipogenic differentiation. Adipocyte, 3(4), 290–296.

Garibyan, L., & Avashia, N. 2013. Research Techniques Made Simple: Polymerase Chain Reaction (PCR). The Journal of Investigative Dermatology, 133(3), e6.

Giralt, M., & Villarroya, F. 2013. White, brown, beige/brite: different adipose cells for different functions?. Endocrinology, 154(9), 2992-3000.

Gould, D. W., Lahart, I., Carmichael, A. R., Koutedakis, Y., & Metsios, G. S. 2013. Cancer cachexia prevention via physical exercise: molecular mechanisms. Journal of cachexia, sarcopenia and muscle, 4(2), 111-124.

Gullett, N. P., Mazurak, V., Hebbar, G., & Ziegler, T. R. 2011. Nutritional interventions for cancer-induced cachexia. Current problems in cancer, 35(2), 58.

Hatakeyama, S., Summermatter, S., Jourdain, M., Melly, S., Minetti, G. C., & Lach-Trifilieff, E. 2016. ActRII blockade protects mice from cancer cachexia and prolongs survival in the presence of anti-cancer treatments. Skeletal Muscle, 6(1), 1.

Henriques, F. S., Sertié, R. A. L., Franco, F. O., Knobl, P., Neves, R. X., Andreotti, S., ... & Batista, M. L. 2017. Early suppression of adipocyte lipid turnover induces immunometabolic modulation in cancer cachexia syndrome. The FASEB Journal, fj-201601151R.

Higami, Y., Barger, J. L., Page, G. P., Allison, D. B., Smith, S. R., Prolla, T. A., & Weindruch, R. 2006. Energy restriction lowers the expression of genes linked to inflammation, the cytoskeleton, the extracellular matrix, and angiogenesis in mouse adipose tissue. The Journal of nutrition, 136(2), 343-352.

Hulmi, J. J., Oliveira, B. M., Silvennoinen, M., Hoogaars, W. M., Ma, H., Pierre, P., ... & Ritvos, O. 2013. Muscle protein synthesis, mTORC1/MAPK/Hippo signaling, and capillary density are altered by blocking of myostatin and activins. American Journal of Physiology-Endocrinology and Metabolism, 304(1), E41-E50.

Jeanson, Y., Carrière, A., & Casteilla, L. 2015. A new role for browning as a redox and stress adaptive mechanism? Frontiers in endocrinology, 6.

Julienne, C. M., Dumas, J. F., Goupille, C., Pinault, M., Berri, C., Collin, A., ... & Servais, S. 2012. Cancer cachexia is associated with a decrease in skeletal muscle mitochondrial oxidative capacities without alteration of ATP production efficiency. Journal of cachexia, sarcopenia and muscle, 3(4), 265-275.

Kershaw, E. E., Schupp, M., Guan, H. P., Gardner, N. P., Lazar, M. A., & Flier, J. S. 2007. PPARγ regulates adipose triglyceride lipase in adipocytes in vitro and in vivo. American Journal of Physiology-Endocrinology and Metabolism,293(6), E1736-E1745.

Kim, S., & Moustaid-Moussa, N. 2000. Secretory, endocrine and autocrine/paracrine function of the adipocyte. The Journal of Nutrition, 130(12), 3110S-3115S.

Kir, S., White, J. P., Kleiner, S., Kazak, L., Cohen, P., Baracos, V. E., & Spiegelman, B. M. 2014. Tumor-derived PTHrP Triggers Adipose Tissue Browning and Cancer Cachexia. Nature, 513(7516), 100–104.

Kleinert, M., Parker, B. L., Chaudhuri, R., Fazakerley, D. J., Serup, A., Thomas, K. C., ... & Jeppesen, J. 2016. mTORC2 and AMPK differentially regulate muscle triglyceride content via Perilipin 3. Molecular Metabolism, 5(8), 646-655.

Kliewer, K. L., Ke, J.-Y., Tian, M., Cole, R. M., Andridge, R. R., & Belury, M. A. 2015. Adipose tissue lipolysis and energy metabolism in early cancer cachexia in mice. Cancer Biology & Therapy, 16(6), 886–897.

Koncarevic, A., Kajimura, S., Cornwall-Brady, M., Andreucci, A., Pullen, A., Sako, D., ... & Howard, E. 2012. A novel therapeutic approach to treating obesity through modulation of TGFβ signaling. Endocrinology, 153(7), 3133-3146.

Kremer, R., Li, J., Camirand, A., & Karaplis, A. C. 2011. Parathyroid hormone related protein (PTHrP) in tumor progression. In Human Cell Transformation (pp. 145-160). Springer New York.

Lee, Y. S., Huynh, T. V., & Lee, S. J. 2016. Paracrine and endocrine modes of myostatin action. Journal of Applied Physiology, 120(6), 592-598.

Levine, J. A. 2002. Non-exercise activity thermogenesis (NEAT). Best Practice & Research Clinical Endocrinology & Metabolism, 16(4), 679-702.

Lipina, C., & Hundal, H. S. 2016. Lipid modulation of skeletal muscle mass and function. Journal of Cachexia, Sarcopenia and Muscle.

Lo, K. A., & Sun, L. 2013. Turning WAT into BAT: a review on regulators controlling the browning of white adipocytes. Bioscience Reports, 33(5), e00065.

Loumaye, A., de Barsy, M., Nachit, M., Lause, P., Frateur, L., van Maanen, A., ... & Thissen, J. P. 2015. Role of activin A and myostatin in human cancer cachexia. The Journal of Clinical Endocrinology & Metabolism, 100(5), 2030-2038.

Ma, Y. J., Yu, J., Xiao, J., & Cao, B. W. 2015. The consumption of omega-3 polyunsaturated fatty acids improves clinical outcomes and prognosis in pancreatic cancer patients: a systematic evaluation. Nutrition and cancer, 67(1), 112-118.

Mahmood, T., & Yang, P. C. 2012. Western blot: technique, theory, and trouble shooting. North American journal of medical sciences, 4(9), 429.

Mantovani, G., Macciò, A., Madeddu, C., Gramignano, G., Lusso, M. R., Serpe, R., ... & Deiana, L. 2006. A phase II study with antioxidants, both in the diet and supplemented, pharmaconutritional support, progestagen, and anti-cyclooxygenase-2 showing efficacy and safety in patients with cancer-related anorexia/cachexia and oxidative stress. Cancer Epidemiology and Prevention Biomarkers, 15(5), 1030-1034.

Moses, A. W. G., Slater, C., Preston, T., Barber, M. D., & Fearon, K. C. H. 2004. Reduced total energy expenditure and physical activity in cachectic patients with pancreatic cancer can be modulated by an energy and protein dense oral supplement enriched with n-3 fatty acids. British journal of cancer, 90(5), 996-1002.

Murphy, K. T., Chee, A., Trieu, J., Naim, T., & Lynch, G. S. 2012. Importance of functional and metabolic impairments in the characterization of the C-26 murine model of cancer cachexia. Disease Models & Mechanisms, 5(4), 533–545.

Müller, T. D., Perez-Tilve, D., Tong, J., Pfluger, P. T., & Tschöp, M. H. 2010. Ghrelin and its potential in the treatment of eating/wasting disorders and cachexia. Journal of cachexia, sarcopenia and muscle, 1(2), 159-167.

Naghavi, M., Wang, H., Lozano, R., Davis, A., Liang, X., Zhou, M., ... & Aziz, M. I. A. 2015. Global, regional, and national age-sex specific all-cause and cause-specific mortality for 240 causes of death, 1990-2013: a systematic analysis for the Global Burden of Disease Study 2013. Lancet, 385(9963), 117-171.

Nissinen, T. A., Degerman, J., Räsänen, M., Poikonen, A. R., Koskinen, S., Mervaala, E., ... & Hulmi, J. J. 2016. Systemic blockade of ACVR2B ligands prevents chemotherapy-induced muscle wasting by restoring muscle protein synthesis without affecting oxidative capacity or atrogenes. Scientific Reports,6.

Orava, J., Nuutila, P., Lidell, M. E., Oikonen, V., Noponen, T., Viljanen, T., ... & Virtanen, K. A. 2011. Different metabolic responses of human brown adipose tissue to activation by cold and insulin. Cell metabolism, 14(2), 272-279.

Penet, M.-F., & Bhujwalla, Z. M. 2015. Cancer Cachexia, Recent Advances, and Future Directions. Cancer Journal (Sudbury, Mass.), 21(2), 117–122.

Petruzzelli, M., Schweiger, M., Schreiber, R., Campos-Olivas, R., Tsoli, M., Allen, J., Swarbrick, M., Rose-John, S., Rincon, M., Robertson, G., Zechner, R & Wagner E. F. 2014. A switch from white to brown fat increases energy expenditure in cancer-associated cachexia. Cell metabolism, 20(3), 433-447.

Petruzzelli, M. & Wagner, EF. 2016. Mechanisms of metabolic dysfunction in cancer-associated cachexia. Genes & Development. 2016;30(5):489-501.

Porporato, P. E. 2016. Understanding cachexia as a cancer metabolism syndrome. Oncogenesis, 5(2), e200.

Qiang, L., Wang, L., Kon, N., Zhao, W., Lee, S., Zhang, Y., ... & Accili, D. 2012. Brown remodeling of white adipose tissue by SirT1-dependent deacetylation of Pparγ. Cell, 150(3), 620-632.

Ramos, S. V., Turnbull, P. C., & MacPherson, R. E. 2016. Adipose tissue depot specific differences of PLIN protein content in endurance trained rats. Adipocyte, 5(2), 212-223.

Rebbapragada, A., Benchabane, H., Wrana, J. L., Celeste, A. J., & Attisano, L. 2003. Myostatin signals through a transforming growth factor β-like signaling pathway to block adipogenesis. Molecular and cellular biology, 23(20), 7230-7242.

Rohm, M., Schäfer, M., Laurent, V., Üstünel, B. E., Niopek, K., Algire, C., ... & Pellegata, N. S. 2016. An AMP-activated protein kinase-stabilizing peptide ameliorates adipose tissue wasting in cancer cachexia in mice. Nature Medicine.

Rydén, M., Agustsson, T., Laurencikiene, J., Britton, T., Sjölin, E., Isaksson, B., ... & Arner, P. 2008. Lipolysis—not inflammation, cell death, or lipogenesis—is involved in adipose tissue loss in cancer cachexia. Cancer, 113(7), 1695-1704.

Sassmann-Schweda, A., Singh, P., Tang, C., Wietelmann, A., Wettschureck, N., & Offermanns, S. 2016. Increased apoptosis and browning of TAK1-deficient adipocytes protects against obesity. JCI insight, 1(7).

Sanchez-Delgado, G., Martinez-Tellez, B., Olza, J., Aguilera, C. M., Gil, A., & Ruiz, J. R. 2015. Role of exercise in the activation of brown adipose tissue. Annals of Nutrition and Metabolism, 67(1), 21-32.

Schiaffino, S., & Reggiani, C. 2011. Fiber types in mammalian skeletal muscles. Physiological reviews, 91(4), 1447-1531.

Schlüter, K. D. 1999. PTH and PTHrP: similar structures but different functions. Physiology, 14(6), 243-249.

Seale, P., Conroe, H. M., Estall, J., Kajimura, S., Frontini, A., Ishibashi, J., ... & Spiegelman, B. M. 2011. Prdm16 determines the thermogenic program of subcutaneous white adipose tissue in mice. The Journal of clinical investigation, 121(1), 96-105.

Segal, R. J., Reid, R. D., Courneya, K. S., Malone, S. C., Parliament, M. B., Scott, C. G., ... & Wells, G. A. 2003. Resistance exercise in men receiving androgen deprivation therapy for prostate cancer. Journal of clinical oncology,21(9), 1653-1659

Segal, R. J., Reid, R. D., Courneya, K. S., Sigal, R. J., Kenny, G. P., Prud'Homme, D. G., ... & Slovinec D'Angelo, M. E. 2009. Randomized controlled trial of resistance or aerobic exercise in men receiving radiation therapy for prostate cancer. Journal of clinical oncology, 27(3), 344-351.

Seldin, M. M., & Wong, G. W. 2012. Regulation of tissue crosstalk by skeletal muscle-derived myonectin and other myokines. Adipocyte, 1(4), 200-202.

Shan, T., Liang, X., Bi, P., & Kuang, S. 2013. Myostatin knockout drives browning of white adipose tissue through activating the AMPK-PGC1α-Fndc5 pathway in muscle. The FASEB Journal, 27(5), 1981-1989.

Sidossis, L., & Kajimura, S. 2015. Brown and beige fat in humans: thermogenic adipocytes that control energy and glucose homeostasis. The Journal of Clinical Investigation, 125(2), 478–486.

Singh, R., Braga, M., & Pervin, S. 2014. Regulation of brown adipocyte metabolism by myostatin/follistatin signaling. Frontiers in cell and developmental biology, 2, 60.

Smith, G. I., Julliand, S., Reeds, D. N., Sinacore, D. R., Klein, S., & Mittendorfer, B. 2015. Fish oil–derived n–3 PUFA therapy increases muscle mass and function in healthy older adults. The American journal of clinical nutrition, 102(1), 115-122.

Stephens, N. A., Skipworth, R. J., MacDonald, A. J., Greig, C. A., Ross, J. A., & Fearon, K. C. 2011. Intramyocellular lipid droplets increase with progression of cachexia in cancer patients. Journal of cachexia, sarcopenia and muscle,2(2), 111-117.

Strasser, F., Palmer, J. L., Schover, L. R., Yusuf, S. W., Pisters, K., Vassilopoulou□Sellin, R., ... & Bruera, E. 2006. The impact of hypogonadism and autonomic dysfunction on fatigue, emotional function, and sexual desire in male patients with advanced cancer. Cancer, 107(12), 2949-2957.

Suzuki, H., Asakawa, A., Amitani, H., Nakamura, N., & Inui, A. 2013. Cancer cachexia—pathophysiology and management. Journal of gastroenterology,48(5), 574-594.

Tisdale, M. J. 1997. Biology of cachexia. Journal of the National Cancer Institute, 89(23), 1763-1773.

Tisdale, M. J. 2010. Reversing cachexia. Cell, 142(4), 511-512.

Thermo Fisher Scientific. 2016. Real-time PCR handbook. Referred 15.2.2017. http://www.thermofisher.com/content/dam/LifeTech/Documents/PDFs/PG1503-PJ9169-CO019861-Update-qPCR-Handbook-branding-Americas-FLR.pdf

Toledo, M., Busquets, S., Sirisi, S., Serpe, R., Orpí, M., Coutinho, J., ... & Argilés, J. M. 2011. Cancer cachexia: physical activity and muscle force in tumour-bearing rats. Oncology reports, 25(1), 189.

Toledo, M., Penna, F., Oliva, F., Luque, M., Betancourt, A., Marmonti, E., ... & Busquets, S. 2015. A multifactorial anti□cachectic approach for cancer cachexia in a rat model undergoing chemotherapy. Journal of cachexia, sarcopenia and muscle.

Tsoli, M., & Robertson, G. 2013. Cancer cachexia: malignant inflammation, tumorkines, and metabolic mayhem. Trends in Endocrinology & Metabolism, 24(4), 174-183.

Tsoli, M., Schweiger, M., Vanniasinghe, A. S., Painter, A., Zechner, R., Clarke, S., & Robertson, G. 2014. Depletion of White Adipose Tissue in Cancer Cachexia Syndrome Is Associated with Inflammatory Signaling and Disrupted Circadian Regulation. PLoS ONE, 9(3), e92966.

Tsoli, M., Swarbrick, M. M., & Robertson, G. R. 2016. Lipolytic and thermogenic depletion of adipose tissue in cancer cachexia. In Seminars in cell & developmental biology (Vol. 54, pp. 68-81). Academic Press.

Tsuchida K. 2014. Myokines and Signal Crosstalk between Skeletal Muscle and Adipose tissue. Austin J Endocrinol Diabetes. 2014;1(3): 1013. ISSN: 2381-9200.

Turner, N., Bruce, C. R., Beale, S. M., Hoehn, K. L., So, T., Rolph, M. S., & Cooney, G. J. 2007. Excess lipid availability increases mitochondrial fatty acid oxidative capacity in muscle. Diabetes, 56(8), 2085-2092.

Van Herpen, N. A., & Schrauwen-Hinderling, V. B. 2008. Lipid accumulation in non-adipose tissue and lipotoxicity. Physiology & behavior, 94(2), 231-241.

Vaughan, V. C., Martin, P., & Lewandowski, P. A. 2013. Cancer cachexia: impact, mechanisms and emerging treatments. Journal of cachexia, sarcopenia and muscle, 4(2), 95-109.

Zhang, C., McFarlane, C., Lokireddy, S., Masuda, S., Ge, X., Gluckman, P. D., ... & Kambadur, R. 2012. Inhibition of myostatin protects against diet-induced obesity by enhancing fatty acid oxidation and promoting a brown adipose phenotype in mice. Diabetologia, 55(1), 183-193.

Zhou, X., Wang, J. L., Lu, J., Song, Y., Kwak, K. S., Jiao, Q., ... & Lacey, D. L. 2010. Reversal of cancer cachexia and muscle wasting by ActRIIB antagonism leads to prolonged survival. Cell, 142(4), 531-543.

APPENDIX. LIST OF THE PRIMARY AND SECONDARY ANTIBODIES USED IN THE STUDY

Protein	Primary ab	Manufacturer	Secondary ab	Manufacturer
ACC*** (1:2000)	Rabbit ab (280 kDa)	Cell Signaling #3676	HRP-conjugated anti-rabbit IgG ab	Jackson ImmunoResearch Laboratories, PA, USA
Phospho-ACC (Ser79)** (1:2000)	Rabbit ab (280 kDa)	Cell Signaling #3661	HRP-conjugated anti-rabbit IgG ab	Jackson ImmunoResearch Laboratories, PA, USA
ATGL** (1:1500)	Rabbit ab (54 kDa)	Cell Signaling #2138	HRP-conjugated anti-rabbit IgG ab	Jackson ImmunoResearch Laboratories, PA, USA
Cyt *c*** (1:1000)	Goat ab (10-15 kDa)	Santa Cruz Biotechnology sc-8385	HRP-conjugated anti-goat IgG ab	Jackson ImmunoResearch Laboratories, PA, USA
α-Tubulin*** (1:3000)	Mouse ab (50 kDa)	Sigma, DM1A-T6199	HRP-conjugated anti-rabbit IgG ab	Jackson ImmunoResearch Laboratories, PA, USA
HSL** (1:1000)	Rabbit ab (81-83 kDa)	Cell Signaling #4107	HRP-conjugated anti-rabbit IgG ab	Jackson ImmunoResearch Laboratories, PA, USA
p-HSL (Ser660)** (1:1000)	Rabbit ab (81-83 kDa)	Cell Signaling #4126	HRP-conjugated anti-rabbit IgG ab	Jackson ImmunoResearch Laboratories, PA, USA
STAT3*** (1:3000)	Mouse ab (79-86 kDa)	Cell Signaling #9139	HRP-conjugated anti-mouse IgG ab	Jackson ImmunoResearch Laboratories, PA, USA
Phospho-STAT3 (Tyr705)*** (1:1000)	Rabbit ab (79-86 kDa)	Cell Signaling #9145	HRP-conjugated anti-rabbit IgG ab	Jackson ImmunoResearch Laboratories, PA, USA
Total OXPHOS (1:1000)	Mouse ab (20-55 kDa)*	Abcam MS604, ab110413*	HRP-conjugated anti-mouse IgG ab	Jackson ImmunoResearch Laboratories, PA, USA
PGC-1α** (1:5000)	Rabbit ab (92-105 kDa)	Calbiochem 516557	HRP-conjugated anti-rabbit IgG ab	Jackson ImmunoResearch Laboratories, PA, USA
PLIN5** (1:3000)	Rabbit ab (50 kDa)	Novus Biologicals NB110-60509	HRP-conjugated anti-rabbit IgG ab	Jackson ImmunoResearch Laboratories, PA, USA
UCP1** (1:3000)	Rabbit ab (32 kDa)	Abcam ab10983	HRP-conjugated anti-rabbit IgG ab	Jackson ImmunoResearch Laboratories, PA, USA

* Total OXPHOS (ab110413) contains five different Abcam mouse antibodies, CI subunit NDUFB8 (ab110242), size 20 kDa, CII-30kDa (ab14714), size 30 kDa, CIII-Core protein 2 (ab14745), size 48 kDa, CIV subunit I (ab14705), size 40 kDa and CV alpha subunit (ab14748), size 55 kDa. All of the antibodies are monoclonal.

** = polyclonal antibody, *** = monoclonal antibody